DEVELOPMENT AND OPTICAL CHARACTERIZATION OF WHITE LIGHT EMISSION ORGANIC NANOMATERIALS

for Master degree in Optics
Advisor: Mario. A. Rodríguez
Thesis presented by Mayra Lucila Melgoza Ramírez

Thanks

This work cannot be possible whitout the support of my advisor PhD. Mario Rodríguez, who helped me an supervased me, I managed to successfully complete my thesis work. I also wanna thanks, my master teaches who gave me the courage to complete my studies and continue in that process knowledge. I want to thank also to the GPOM group where I had great memories and great friendships, I would like to thank you for everything. This work was partially supported by CONACyT (Masters scholarship and basic science project 183147) so I want to say thanks.

I say thanks, to my parents for all love and support, that they have given me over the years, and that even in the hard times have encouraged me to keep going. Their courage and conviction inspire me always to follow. To my brothers and syster, who have been by my side at all times and with whom I spent pleasant moments and love them. It is they whom I dedicate this work.

Contents

List of Figures

List of Tables

Abstract

Organic materials have been the focus of a growing body academic and industry fields for more than 50 years. Up to only a short time ago, organic electronic and optical phenomena have been the domain of pure research, somewhat removed from practical application. Since the first demonstration in mid-1980s, with a low voltage and efficient thin film light emitting diode by Ching Tang and Steven van Slyke at Kodak [1], organic materials have proven useful in a number of applications. Some of these applications are organic light emitter diodes (OLEDs), photovoltaic devices (OPVs), sensors and biomedical, among others. In this thesis, organic fluorophores BT3, ACN1, BT2, BT20 and DBBT3-Hex with blue, green and red were processed as organic nanoparticles (ONPs) and doped silica nanoparticles (SNPs) by reprecipitation and microemulsion techniques. Electronic molecular transitions for BT3, ACN1, BT2, BT20 and DBBT3-Hex were calculated by theoretical methods and also was established the molecular electronic density distribution on frontier orbitals and bandgap data. Linear optical properties and morphological characteristics for aqueous suspension of each nanomaterials were established by absorption spectroscopy, photoluminescence, quantum efficiency measurements, dynamic light scattering (DLS) and scanning electron microscopy (SEM). SNPs fabricated in this work showed a narrow size distribution, around of 48.8±4.11 which was observed by SEM images and confirmed with DLS measurement, while a wide size distribution (around 43.8±21.88) was denoted for the nanomaterials fabricated by reprecipitation. Molar ratios of these five organic materials in solution and aqueous suspension were combined to obtain mixtures red-green-blue (RGB) with white-light emission that was corroborated by determination of color coordinates of the Commission Internationale de L'eclairage (CIE). Solution with white-light emission by excitation

at 375 nm was fabricated by molar ratio of R:G:B = 0.5:1.5:2 with color coordinates of (0.29, 0.30). In the solid state, fabricated aqueous suspension RGB of NPs present (0.35, 0.38), and in the case of SNPs the coordinates were (0.21, 0.35).

Chapter 1

Introduction

During the last decade, fluorescent nanoparticle (FNPs) systems have appeared as novel functional materials in several areas as biology, chemistry, material science, optics, photovoltaic cells and biomedicine due to possible applications [2–4]. These organic and inorganic FNPs are robust and can be surface-modified, however, emission of organic system has the advantage to be tunable-emission by chemical structural modification. There are a great of organic fluorophores that have been used in the fabrication of nanoparticles [5], which include small organic dyes [6], metal-ligand complexes [7, 8], hydrophilic polymers (hydrogels) [9, 10], hydrophobic organic polymers [11], biological compounds and genetically encoded fluorescent proteins [12]. Although it is noteworthy that the inorganic nanoparticles (INPs) have excellent photoluminescence properties, they also proven to be highly toxic to living tissue and sometimes difficulties with respect to surface modification. Situation that promotes the interest in study and fabrication of fluorescent nanoparticles based on organic molecules, which might be easily chemically modified to enhance their photophysical properties [13]. In addition, the optical and electronic properties in organic nanomaterials depends on the intermolecular interactions of weak types, such as hydrogen bonds, $\pi - \pi$ stacking, Van der Waals contacts, and charge transfer (CT) interactions [14]. A key to the design of high performance optical and electronic organic devices is the understanding of the electronic structure of molecular structures. In general, is well known that changes in structure or composition of an organic material can markedly alter its bulk properties (optical, chemical, me-

chanical and physiochemical). The use of organic compounds as active materials in electronic and optoelectronic devices opens the opportunity to develop the design and study of these materials for a large number of applications [15]. In particular, in photonics and biophotonics fields the interest for organic fluorophores is justified by the fact that organic compounds offer a lot of species and are less cytotoxic for biological tissue, these have fluorescence quantum yields that are high in the visible light range, ONPs have mayor reproducibility, the fluorescence lifetimes of organic molecules are bigger than quantum dots (QDs), making these molecules suitable for applications involving lifetime measurements [5]. Recently, a large number of scientific and technological groups are developing new nanomaterials with white-emission, for possible applications in flexible full-color OLEDs, in backlights for liquid crystalline displays, bio-imaging to chemo- and biosensors. [16–18]. However, reports of white-light emitting organic nanoparticles are very rare in the literature. The other important approach is that ONPs can be fabricated by several methods, that are very simple and with low economical cost [19]. Moreover, by microemulsion methods is possible covering the nanoparticles with silica increasing their photo-stability, easy surface functionalization and decreasing the cytotoxicity, which has attracted increasing attention in biomedical research [20]. Perspectives for the future development of organic fluorescent nanoparticles is for bioimaging applications in particular to decipher multiple biological events simultaneously [21, 22] or photodynamic therapy, e. g. modified silica nanoparticles (SNPs), co-encapsulating a photosensitizing drug [23, 24].

In particular, an ideal white light emitter materials demands simultaneous emission on red, green and blue color with nearly similar distribution of intensities covering the whole region of visible spectra [25, 26]. The designs of organic white light emitters cover a large area of chemistry and this is based on some process as from energy transfer [27–29] where the interactions between blue, green and red fluorophores often results in Förster resonance energy transfer (FRET) process improving emission from the red-emitting fluorescent units which act as the energy acceptors and producing white-light emission. Other literature reports of white-light emissive molecules are reported by simple protonation of species [30], here the optical behavior of the

fluorophores depend whether they are in a basic or acid pH solution. In this way, fluorophore with large spectral widths and considerably different emission features in neutral and protonated (or deprotonated) forms can show full color RGB luminescence at precisely optimized conditions. It has also been reported white-light emitters organic materials by designed self-assembly [31], by weak bonding interactions, resulting in broad emission profiles and in some cases, white-light is produced after they are aggregated. [16, 32] Herein, we report the fabrication and photo-physical characterization of molecules derivatives from benzothiadazole (ACN1, BT2, BT20 and DBBT3-Hex) and derivatives from fluorene (BT3). These substances are highly fluorescent in solution and exhibit emission band in the blue, blue-green, yellow and red region. The goal of our work is obtaining aqueous suspension of nanomaterials with white light-emission, for this, firstly were performed RGB mixtures in solution for BT3:ACN1:DBBT3-Hex (RGB1) and BT3:BT2:BT20 (RGBBTs) subsequently were fabricated the RGB NPs by reprecipitation and microemulsion methods. Their optical properties for these fluorophores were evaluated and compared with those obtained in solution.

Chapter 2

Justification

During last decade there are a great number of applications for organic materials such as sensors, solar cells and organics field effect transistor (OFETs) [33–37], the attraction of this field has been the fact that organic compounds offer a variety of species and can be modify structurally in ways to impact their properties. Situation that have been stimulated the research of new organic materials, where design and study of their properties are essential for the development of these systems. Moreover, increasing interest has been devoted to organic fluorescent nanoparticles for applications as key components in display and lighting devices based on OLEDs, biological imaging and photo-therapy [24, 38, 39]. Actually, organic nanoparticles show an enhanced stability toward light and oxygen compared to isolated molecules, appearing to be good candidates for many applications that involve interactions with light [38]. White light-emitting organic materials have gained much attention owing to their great potential for practical lighting applications, enhanced the brightness of the fluorophore and as multiplex bioanalysis and molecular imaging [32, 40, 41]. In this work we develop the fabrication of organic nanomaterials with white light-emission, through mixing three compounds that possess highly photoluminescence in blue, green and red, by two methods: reprecipitation and microemulsion, the methods used are inexpensive and easy to manufacture. Although, by the microemulsion method ONPs can be coated with silica increasing their photo-stability, uniformity in size, easy surface functionalization and biocompatibility, which have attracted increasing attention in biomedical research. The perspectives for the future de-

velopment of organic nanoparticles for bioimaging to decipher multiple biological events simultaneously [21] using FRET-mediated emission signatures can be tuned to have the nanoparticles to exhibit multiple colors under one single wavelength excitation [22].

2.1 Objectives

1. To develop a family of highly fluorescent organic materials.
2. To develop methodology for the manufacture of fluorescent organic nanoparticles whit a dispersion of small size and white light emission.
3. Perform characterization of photophysical properties of the materials in solution and nanostructure.
4. To study the structure-property relationship in these materials and their possible applications.

2.2 Goals

- Fabrication of nanomaterials, mixing five different organic molecules (BT3, ACN1, BT2, BT20 and DBBT3-Hex), and obtain white light-emission. And with this, to establish the relationship between structure and photophysical properties of these materials.

Chapter 3

Theory

3.1 Electronic transitions of organic compounds

Organic molecules containing electron orbital π type in their structure, that means, which contain double bonds, exhibit unique properties due to the high mobility of the electrons in the system. The most important feature from these molecules is their intense absorption in the ultraviolet-visible regimen of the electromagnetic spectrum which causes electronic transitions that produce excited states, as shown in Fig. 3.1. From these energy states the electrons decay to basal states through various mechanisms relaxation, either non-radiative, that is to say, no light is emitted state but excited decays through vibrational and rotational mechanisms or through radiative relaxation, by photons emission (luminescence).

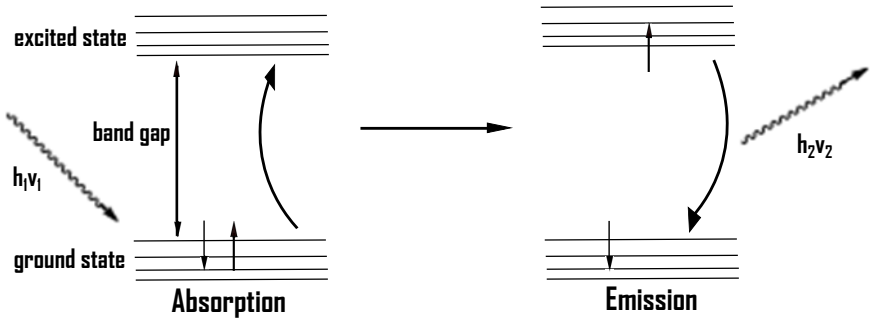

Figure 3.1: Electronic phenomena caused by the absorption of photons.

Through of molecular engineering is possible to orientate the relaxation process to specific relaxation mechanism, for example, with the insertion of particular fragments into the molecular structure which are known as fluorophores that are the responsible to the photoluminescence properties, while the alkyl chains favor vibrational relaxation [42, 43]. Additionally, the presence of certain molecular fragment in the structure helps to tune the emission band [44–46]. The mechanistic to control the position of the emission band is the inclusion of electron-donors or –acceptor groups that promotes a change of the occupied and empty energy levels (HOMO and LUMO). In this point is necessary to mention that there are different transitions observed in organic compound that involve bonding electrons σ or π, or n-electrons. The possible electronic transitions for organic compounds are: $\sigma \rightarrow \sigma^*$, these transitions requiere energy from the UV region to promote an electron to the excitate state. Other type of transitions which occur are $n \rightarrow \sigma^*$, these transitions derived from the promotion of an electron of orbital called n to σ^*, this is observed due to presence of the atoms O, N, S, Cl atoms, these transitions have a moderate intensity, because the probability that happen are less likely to occur earlier. The transitions from $n \rightarrow \pi^*$ are of low intensity and are transitions from an electronic orbital n to other one of antibonding π^*. Finally transitions type $\pi \rightarrow \pi^*$ systems, which have alternating double and single bonds in its carbon structure.

3.1.1 Fluorescence phenomenon

The luminescence is the emission of light from any substance, and comes from the excited states of the compound. Luminescence is divided into fluorescence and phosphorescence, depending on the nature of the excited state Fig. 3.3. In a singlet excited state, the electron is unpaired (with opposite spin) to the second electron is located in the ground state. Therefore it back to the ground state is rapidly rotated results in the emission of a photon. The fluorescence emission rates are typically $108s^{-1}$, so that a life time of fluorescence is typical about 10 ns (10×10^{-9} s). The phenomenon of fluorescence is typically present on molecules that are aromatic. Some common fluorescent substances are shown in Figure 3.2.

The phosphorescence is the emission of light from triplet excited states, in which

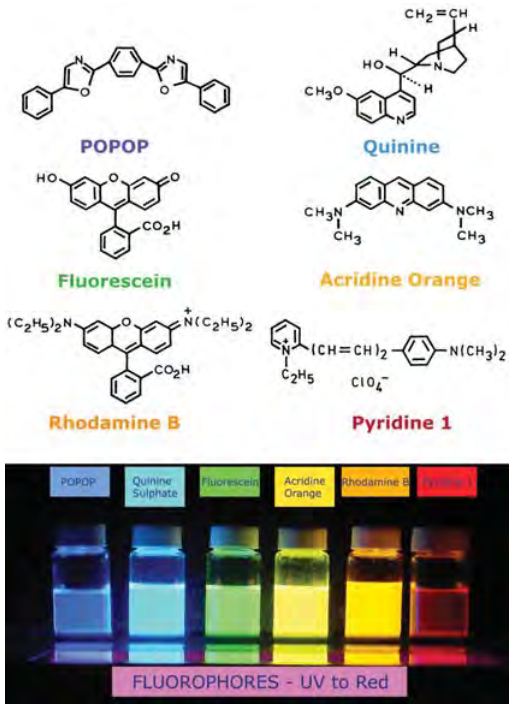

Figure 3.2: Best known structures of fluorescent substances (taken from [49]).

the electron in the excited state has the same spin orientation as the electron in ground states. Transitions to the ground state are forbidden and emission rates are slow (10^3 a 100 s^{-1}), the lifetime of phosphorescence are around of milliseconds to seconds. Photoluminescence emission and excitation studies showed that the photophysical properties strongly depends on the supramolecular structure of the π conjugated backbone. Supramolecular order plays a critical role in device performance, as both charge mobility and luminescent efficiency are influenced by molecular aggregation and structural defects [47]. One fluorescence characteristic is the stokes shift, where the emission is lower than the absorption. Therefore, the fluorescence occurs at lower energies and longer wavelengths. The loss of energy between the energy of excitation and emission are observed universally for fluorescent molecules in solution. A common cause of Stokes shift is the rapid decay to lower energy levels S_1, Fig. 3.3. In addition to this, the fluorophores may show a shift due to effects of solvent, in the excited state reactions, formation of complexes, or energy transfer. One way of determining the Stokes shift, is through the equation (3.1). Where $\tilde{\nu}_{abs}$

and $\tilde{\nu}_{em}$ correspond to absorption and emission wavenumber, respectively.

$$Stokes \;\; shift = \frac{\tilde{\nu}_{em} - \tilde{\nu}_{abs}}{\tilde{\nu}_{abs} * \tilde{\nu}_{em}} \tag{3.1}$$

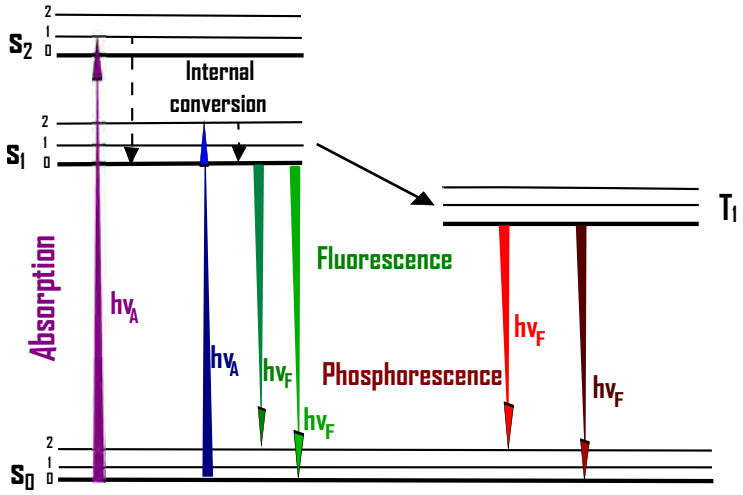

Figure 3.3: Jablonski diagram.

Another property of the fluorescence are the similarities between the emission spectrum and absorption spectrum. This is known as Kasha's rule, generally the symmetry of spectrum is the result of the same transition involved between the absorption and emission, and the vibrational energy is similar to the energy levels of S_0 y S_1.

The quantum yield being the most important feature of a fluorophore last. The quantum yield is the number of photons emitted by the number of absorbed photons [48].

$$\phi = \frac{\#\;\; emitted \;\; photons}{\#\;\; absorbed \;\; photons} \tag{3.2}$$

Substances with high quantum yields, close to unity, such as rhodamine, show a very intense emission [49]. For photoluminescent species, the quantum yield (QY) of its luminescence is a basic property, and its measurement is an important step in the characterization of the species. According to the definition of the QY, only

two quantities need to be known, the number of photons absorbed and the number of photons emitted per unit of time. Unfortunately, reliable measurements of these quantities can be hard to obtain. Here, were considered the easiest situation, namely, for species in dilute solution. In this case, it is customary to measure the fluorescence spectrum and compare its integrated intensity with the same quantity for a reference system with a known QY. This measurement can be done using standard absorption and emission spectrometers.

The QY can be calculated from eq. (3.3):

$$\phi_f^s = \phi_f^r \frac{A_r(\lambda) F_s n_s^2}{A_s(\lambda) F_r n_r^2} \tag{3.3}$$

where ϕ_f^s and ϕ_f^r are the photoluminescence QY of the sample and the standard, respectively. $A_s(\lambda)$ and $A_r(\lambda)$ are the absorption of the solution at the excitation wavelength; F_s and F_r is the fluorescence integral; the refractive indexes of the sample and reference solution are n_s and n_r, respectively. In principle, excitation wavelengths for sample and reference can be different, but this is generally not advisable because it introduces an additional uncertainty in the relative photon flux at the two wavelengths.

3.2 Nanoparticle manufacturing methods

The importance of manufacturing nanomaterials relies on the interesting properties which show in aggregate, with dimensions in the range of about 10 nm to few hundred nanometers [47]. The main advantage of nanomaterials are their specific physical (optical, magnetic, optoelectronic), chemical (reaction activity, catalytic), and biomedical (curing, delivery) properties, opening infinity of opportunities in many fields. There are different methods of synthesis for obtain ONPs, one of these methods is laser ablation [50, 51], in which an intense laser pulses is incident on the organic microcrystals or amorphous material inducing their fragmentation. Nanoparticles size is controlled by establishing the chemical and physics parameters such as solvent concentration, temperature, wavelength and intensity of laser radiation [52–54]. Other technique widely used is the reprecipitation, due to their low cost and it

is not required sophisticated equipment, so that provides a very simple and versatile way to prepare organic nanoparticle dispersions. Reprecipitation method was first reported by Nakanishi and co-workers in 1992, they synthesized organic microcrystals of several chromophores. The method consists mainly in manufacturing aqueous suspensions from a solution of the molecule, the required elements are: i) organic molecule (insoluble in water), ii) a water miscible organic solvent iii) deionized water and iv) surfactant. The method involves a rapid mixing of a small amount of concentrated stock solution of the target compound dissolved in a good solvent with excess of a poor solvent, that get usually a surfactant, should be performed quickly and whit vigorous stirring order to obtain a colloidal suspension, this is accomplished usually in an ultrasonic bath. The great disparity between the solubility of the target compound in the good and poor solvents and the good compatibility of the two solvents are essential for this method. The organic solvent used during the fabrication of nanomaterials is evaporated by vacuum, and the formation of nanoparticules is accelerated. In this methodology is important that the materials used must be highly hydrophobics to promote the formation of small aggregates in a aqueous media stabilized by the surfactant (Fig. 3.4). The size of the NPs can be manipulated by controlling some important parameters of the synthesis such as: a) molecule concentration, b) surfactant concentration, the amount of the injected solution and the aging time of the suspension.

By this method is quickly and easy produce NPs, but in the other hand, the large size distribution of the NPs, due to the heterogeneous environment in which are found, it becomes difficult precisely control the nucleation process and growth. Consequently, the broad size and shape distribution of the ONPs prepared by this method prevents them from has a better self-organization. Moreover, the most important disadvantage is that, the ONPs sometimes are no stable to biological environmental. In this way, other methods of synthesis as microemulsion where it is possible to coat the nanoparticles with silica, which reduce the interaction with the medium.

Microemulsion are colloidal 'nano-dispersions' of water in oil (or oil in water) sta-

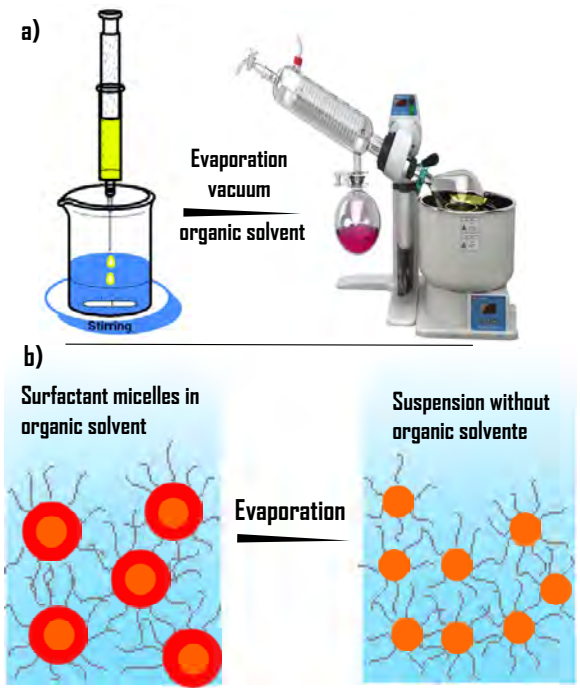

Figure 3.4: Reprecipitation method: a) scheme; b) mechanism.

bilized by a surfactant. These thermodynamically stable dispersions can be considered as nanoreactors which can be used to carry out chemical reactions to synthesize nanomaterials, moreover by means of this technique it is possible to form of different kind of core-shell structures of Organic/Inorganic composites, the structures reported with this configurations have been employed in biological applications owing to their biocompatibility and photo-stability [55, 56]. The microemulsion technique promises to be one of the versatile preparation method which enables to control the particle properties such as mechanisms of particle size control, geometry, morphology, homogeneity and surface area [57]. This method consists in mixing of an oil phase with an aqueous phase or vice versa, oil or aqueous droplets are formed by stirring Fig. 3.5. Generally, the shape (and size) of the dispersed nanodroplets depends mainly by the curvature free energy and is determined by the elastic constant and the curvatures of the surfactant, these nanodroplets have been used to prepare nanoparticles of different kind of materials, where the size and principally the shape of these nanodroplets could template the synthesis of nanomaterials [58], however, the size of nanoparticles is controlled by parameters such as concentration of the organic molecules and the

diameter of the water cores which is related to the ratio R = $[H_2O]$/[surfactant], or changing the type of agitation (mechanical or ultrasonic) [59].

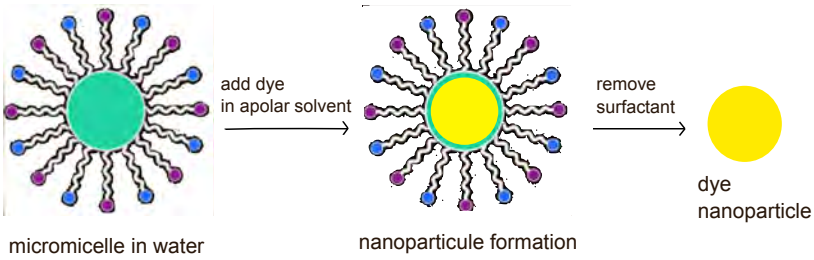

Figure 3.5: Schematic representation of the fabrication of organic nanoparticles.

Moreover, in the case of organic nanoparticles are fascinating as their size-dependent optical properties on absorption and emission [47]. The electronic properties of organic nanoparticles differ fundamentally from inorganic analogous, because each molecule is linked by weak intermolecular forces of Van der Waals type or hydrogen bonding.

3.2.1 Techniques for generating white light

Organic compounds that have emission in red, green and blue are used to obtain white light emission because is possible to tune the wavelength and higher brightness [41], these compounds are found applications as a white organic light emission diodes (WOLEDs) [60], such materials can be used in biological applications as markers or contrast agents. The white light emission can be accomplished by mixing and tuning the three primary color red, blue and green, other way is using the complementary colors, such as cyan and yellow [21]. There are almost two methods for generate a color: The first is called additive process which adds the bands of visible light in a single stimulus color. This method combining red, green and blue primary colors, these combination produce the white color, also can be obtained through the secondary colors (such as magenta, cyan and yellow). The second method is the subtractive process occurs when one or more spectral components are removed from the incident light by absorption and scattering phenomena. The resulting wave-

length which is reflected in a surface produces the sensation of color. Fig. 3.6 [61, 62].

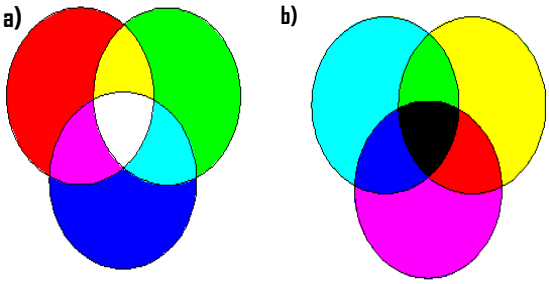

Figure 3.6: a) additive mixture; b) subtractive mixture.

Furthermore, for indoor artificial lighting is possible to generate light of various colors including white. The technique known as RGB is based on the combination of red, green and blue is used for obtains the white (a) Fig. 3.6).

3.3 Applications of organic white light emitting materials

Developments of organic white light emitting materials whit high outputs still remain a relatively explored area. Recent studies have led to better understanding of the properties of such RGB-emitting materials to obtain white photoluminescent materials. Unfortunately in many cases, the generation of white light is limited in solution turning them unsuitable in practical applications, now have been studied the possibility to obtained them in solid-state. At present fluorescent organic nanoparticles have found applications in the field of artificial lighting, displays systems and fluorescent bio-medical tools (bio-imaging by using one or two photon absorption properties [23]). Organic materials are generally preferred about their inorganic counterparts because its low cost, ease of fine-tuning, low toxicity and enough flexibility for device fabrications [25, 32]. Current trends in organic-lighting have boosted the demand for white emitting materials to fabricate efficient lighting devices such as LCD (liquid-crystal display) and OLEDs, and more recently

the WOLEDs. Now, OLED technologies can be founded commercially by General Electric and other companies increasing the demand for successful developments of organic white-light emitting systems [63]; this technology will continue to inspire scientists and designers to explore the potential of prototype products and subsequently introduce to trade. Such is the case of Junhong Zhou, et al. whom developed a simple, low cost, and scalable process based on sandblasting to modify the OLED substrate's surface, the realize a rough surface on a 3.5 inch (Fig. 3.7) white lighting panel demonstrating the possibility manufacturing scalability of the sandblasting technique [18].

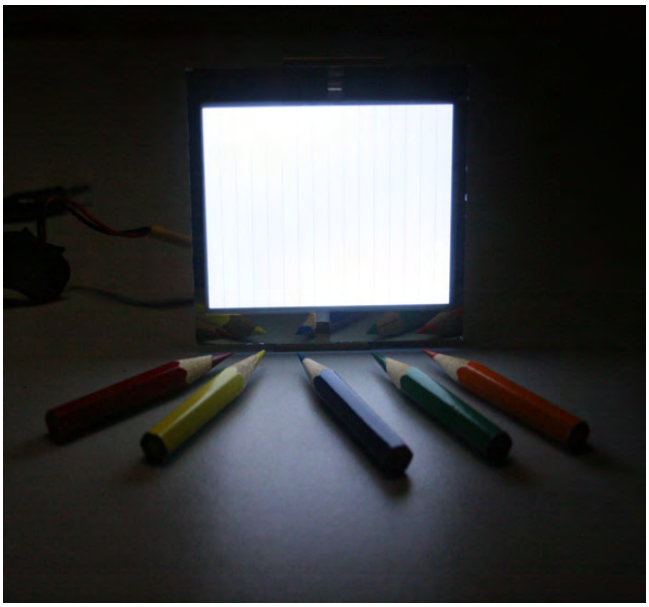

Figure 3.7: The picture of a 3.5 inch white light panel. Taken of [18]

Should be mentioned that, this area has been found considerable progress due to the usage of phosphorescent and inorganic materials, Su-Hua Yang et al. reported a fluorescent-phosphorescent hybrid emission layers (EMLs) these were used to enhance the luminance and stability of the devices, which have blue-EML/CBP inter layer/green-EML/phosphorescent-sensitized-EML/red-EML structures. Good color tunability was achieved for the white OLEDs; the chromatic coordinates were (0.300,0.398) to cold white (0.261,0.367) depending from the applied voltage [60].

Other way to obtain white light emitting materials have been fabricate composites with organic compounds and QDs, this combinations combine the desired properties from both components, thus creating the new properties that may not be present in each individual material. Bingxin Liu et al. synthesized a white light emitting polymer nanocomposites (P-NCs) with color coordinates (0.32, 0.34), using a novel fluorescent polymer and 5-(2-methacryloylethyloxymethyl)-8-quinolinol (MQ) these materials were dispersed in vinyl monomers containing CdSe/ZnS NCs, for tune the white light of material the ratios between P-NCs/MQ were changed [40]. Further important use with fluorescent organic compounds is in biomedicine because is possible incorporate different functional groups allow make them selective to certain types of cells e. g. cancer cells [24, 64]. Furthermore, these materials can be designed to a specific target such as biomolecules and organelles within the cells [23].

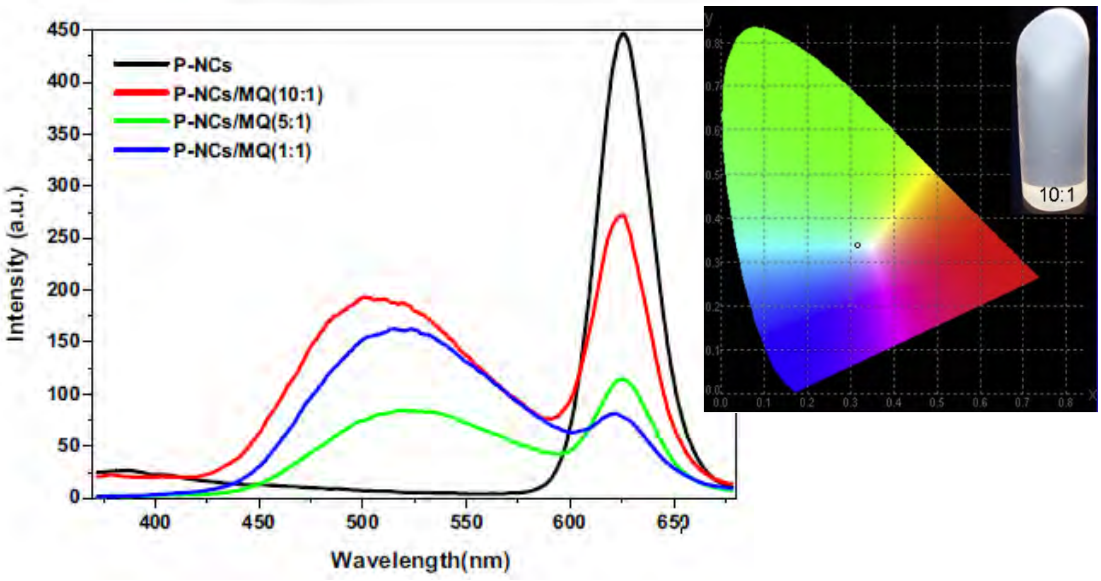

Figure 3.8: PL spectra of P-NCs, P-NCs/MQ(10:1), P-NCs/MQ(5:1) and P-NCs/MQ(1:1), on the left diagram coordinates of P-NCs/MQ(10:1) and imagen under UV ilumination. Imagen taken of [40].

Other fabrication technique is based on the incorporation of fluorescent dyes inside the nanoparticles during the synthetic procedure [24]. Combining organic and inorganic components, such as dye doped silica nanoparticles, often show improved

photostability and higher brightness as compared to fluorescent molecules. This new developed which involve hybrid nanoparticles with organic fluorescent core and biocompatible inorganic as the encapsulation matrix have emerged as a new generation of promising probes for in vivo applications. Regarding, SNPs can achieved with the presence of suitable functional groups e.g. alkoxysilanes, where organic dyes could doped or coated SNPs depending on the desired application or inside the SNP cores. More recently various scientific groups have been incorporated multiple dyes in one nanoparticle, which allows the formation of ultrabright nanoparticles for bio-imaging application to decipher multiple biological events simultaneously [21, 29]. For bio imaging application Audebert et al. demonstrated the preparation of fluorescent white-light emitting SNPs (Fig. 3.9) using only two dye constituents, Naphthalimide (Napht) and tetrazine (Tz) derivatives, furthermore the compound naphthalimide increase their emission when form excimer, and the emission suffers a shift to longer wavelengths [29].

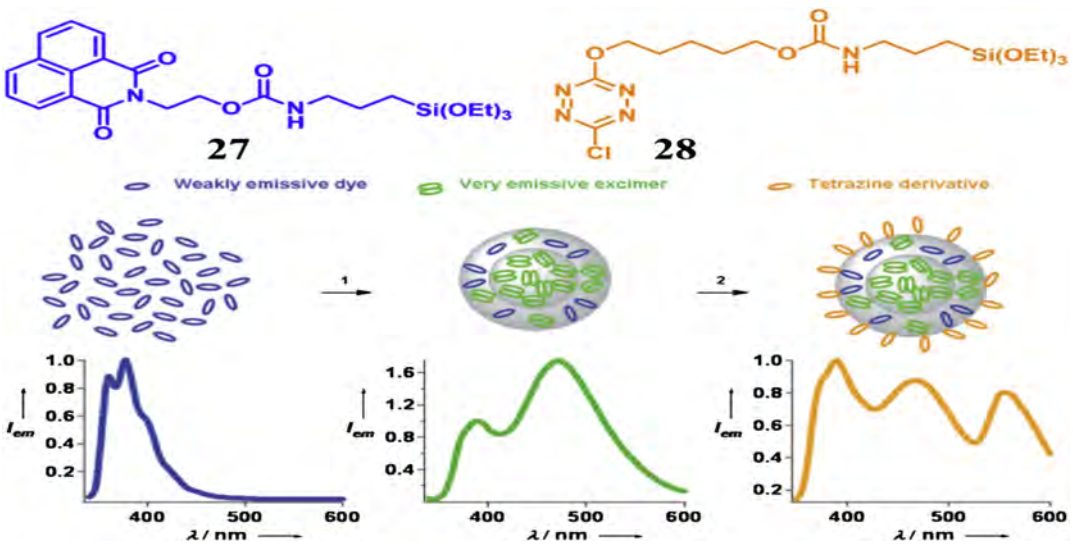

Figure 3.9: Representation of the co-grafting process: 1) formation of NP0; 2) Tz grafting reaction. Emission spectra (λ_{exc}=330 nm) of Napht (blue), NP0 (green), and NPB (orange). Taken of [29].

In general, FRET and other energy transfer processes can become dominant in close proximity resulting in high intense emission from acceptor molecules at the

cost of the emission intensity of the donor molecules. Further, at the surface, energy transfer from the blue emissive NP to the yellow emissive tetrazenes further brightens the yellow emission bands arising from SNP surface. With an increasing quantity of tetrazine grafted, the nanoparticle gradually changes their photoluminescence to a pure white emission (x=0.29, y=0.32).

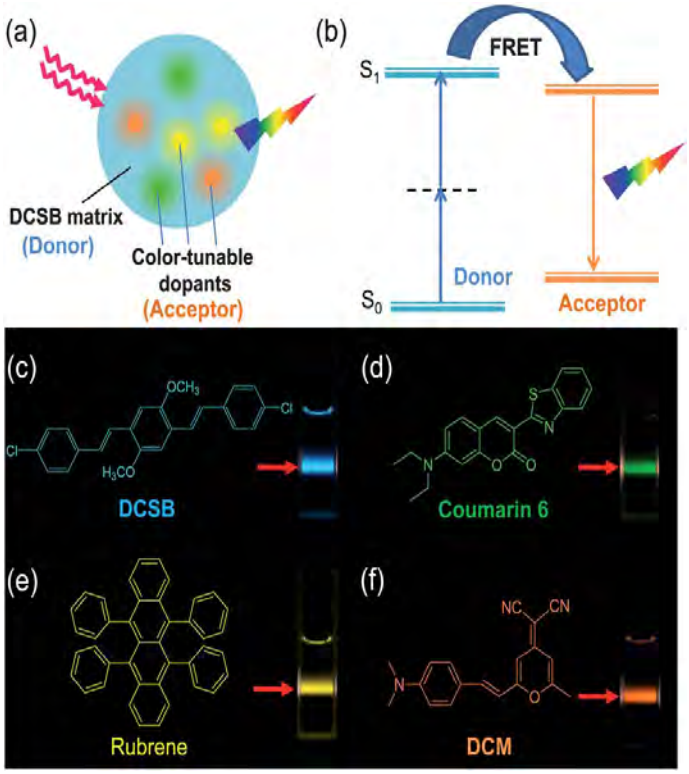

Figure 3.10: (a) Schematic illustration of ONPs comprising of a TPEF matrix of 1,4-dimethoxy-2,5-bis(40-dichlorstyryl) benzene (DCSB) doped with dyes that emit photons of different colors. (b) FRET energy diagram from the DCSB donor to the dye acceptor. (c) Photograph of TPEF matrix of DCSB doped in a THF–water ¼ 1 : 9 (v/v) mixture (blue). (d–f) Photographs of aqueous dispersions of TPEF ONPs. All the doped ONPs dispersed in the THF–water ¼ 1 : 9 (v/v) mixture. The red arrows in (c–f) show 800 nm laser excitation. Taken of [41].

Two years ago, Zhenzhen Xu et al., preparate fluorescent white-light emitting SNPs using dyes fluorescents commercially available doped in a two-photon excited fluorescence (TPEF) host matrix Fig. 3.10. They demonstrated that FRET can

enable highly emissive, photo-stable, low cytotoxicity and full-color tunable TPEF ONPs for bio-labeling and imaging applications [41]. The brightness of the color tunable ONPs which they can obtain was 4 orders of magnitude higher than conventional fluorescent dyes and 3 orders of magnitude higher than quantum dots, and ONPs exhibit TPEF action cross-sections of $\approx$ 1000 GM in the full color-tunable range.

Chapter 4

Experimental

4.1 Materials

Molecules ACN1 (reported by Tsutomu Ishi-i, et. al [65]), BT3 and BT2 (reported by Jesús Rodríguez, et. al [66]), DBBT3-Hex and BT20 were synthesized in our laboratory by palladium cross coupling reactions from benzothiadiazol derivatives and fluorene moieties, their molecular structures are showed in Fig. 4.1. All starting materials and solvents used for synthesis and optical characterization were purchased from Sigma-Aldrich Company, these were employed without previous purification process.

4.2 Instruments

Absorptions spectra in solution and nanoparticles were obtained by using a Perkin Elmer LAMBDA 900 UV/Vis/NIR spectrophotometer. The emission spectra of solutions, suspension (NPs) and silica nanoparticles (SNPs) were measured on Ocean optics USB4000 spectrometer using as excitation source a diode laser of 375 nm. The particle size distributions were measured in a Dynamic light scattering (DLS) with a scattering angle of 173° (Malvern, Zetasizer Nanoscrips). To observe the surface morphology of the NPs and SNPs were used Scanning electron microscope (SEM JEOL-JSM-7800F) and transmission electron microscope (TEM JEOL-1230). By

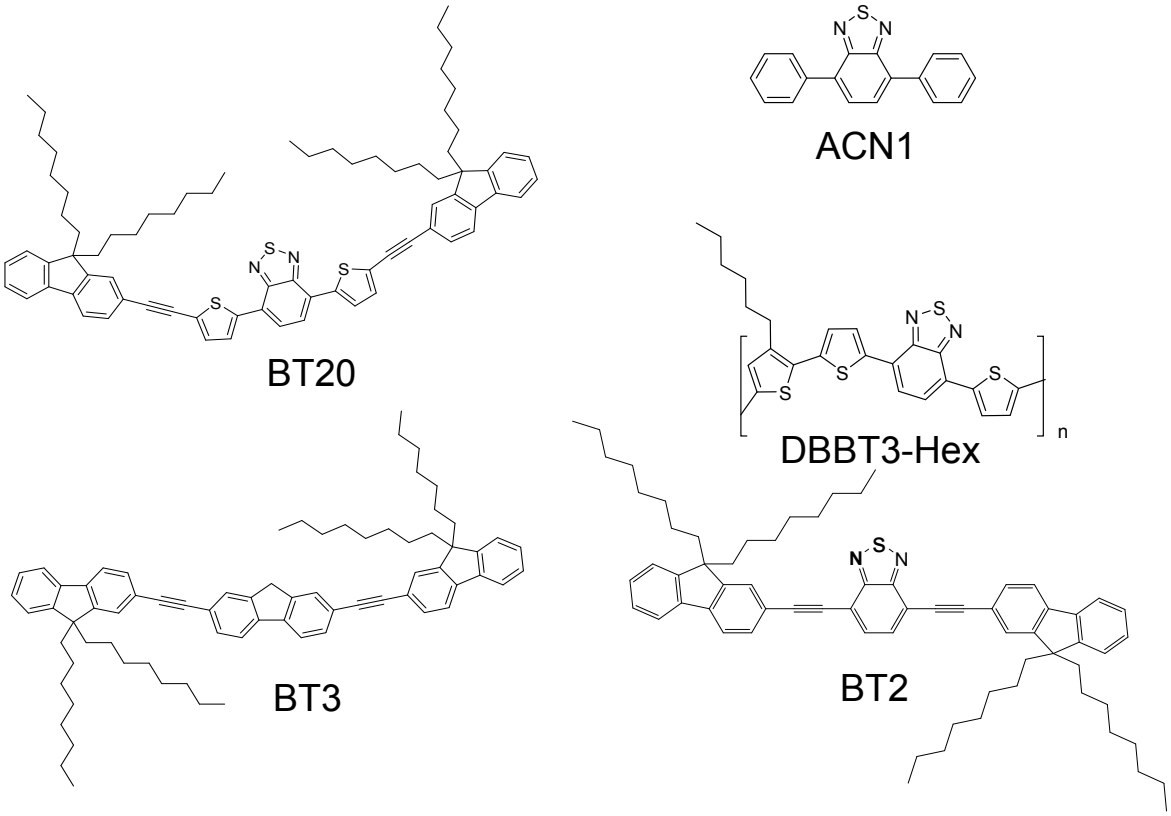

Figure 4.1: Chemical structure of molecules.

using theoretical methods were calculated the HOMO-LUMO energy levels through GAUSSIAN 09 using the B3LYP functional and the bases used were 6-31G for all atoms [67–72]. HOMO and LUMO levels were determined experimentally by cyclic voltammetry (CV) the experiments were carried out by using an advanced electrochemical system, PARSTAT 2273 potentiostat. CV experiment can be done using three electrodes consisting of a working electrode (Pt), a counter electrode (Pt in filament) and a reference electrode ($Ag/AgNO_3$). Silver is used in this experiment as a known reference to calculate the E_{ox} or E_{red}. The estimations can be done with the empirical relation $E_{LUMO} = [-(E_{red}+4.4)+0.22]$ eV or $E_{HOMO} = [-(E_{ox}+4.4)+0.22]$ eV. The quantum yields were obtained by an integrating sphere and using as excitation source a diode laser (Central wavelength 375 nm). The fluorescence quantum yields of samples were measured in solution and solid state (NPs, and SNPs), for DBBT3-Hex and BT20 were used as reference Rhodamine 6G ($\phi_{ref} = 0.89$) [73] dis-

solved in ethanol and for the samples BT3, ACN1 and BT2 were used as reference quinine sulfate (QS) (ϕ_{ref}=0.6) [74] dissolved in water at 0.05 M sulfuric acid. The color coordinates were calculated such as established by the CIE for a light source (Appendix A) [61].

4.3 Preparation of aqueous suspension of organic NPs and SNPs

NPs from compounds BT3, ACN1, BT2, BT20 and DBBT3-Hex, were prepared by using typical reprecipitation method (molecular selfaggregation) [14, 75–77], a briefly description, a small volumes of THF solution were injected into aqueous solution of Cetyltrimethylammonium bromide (CTAB) at concentration of 8×10^4M under ultrasonic agitation, the CTAB is used to avoid coalescence of NPs. THF solvent was removed from the NP system to reduce the exchange degree of the dynamic equilibrium from the isolate molecules to NPs, moreover, the effect of the hydrophobic environment on the NPs was also considered.

To obtain white light-emitting nanomaterials from RGB1-BT3:ACN1:DBBT3-Hex and RGBBTs-BT3:BT2:BT20 by reprecipitacion method first, were prepared a yellow suspension by combining DBBT3-hex:ACN1 and BT20:BT20, then BT3 in solution were added until obtain white light, the molar ratio for white light emitter were was 0.5:1:2 and 1:1:2 respectively. For RGB suspension also was used CTAB as surfactant at concentration of $8 \times 10^4 M$ and was maintained on magnetic stirring all the time during the manufacturing process.

SNPs were synthesized according to methods described by L. Aparicio-Ixta et al. [78]. The method consist in prepared microemulsions by dissolving Aerosol-OT, 1-butanol and NMP in deionized water. Then, the molecule is dissolved in N-Methylpyrrolidone (NMP) and added to the micellar solution under constant magnetic stirring, after half an hour the vinyltriethoxysilane (VTES) is added and the silica nanoparticules (SNPs) are formed, afterwards was added (3-Aminopropyl) tri-

ethoxysilane (APTES) to precipitate the particles and modify the surface of the SNPs with amine groups (NH_2), the solution is kept in stirring vigorously for 20 hours. This methodology is carried out at room temperature. Finally, to remove as much as possible surfactant eliminated the larger NPs, these suspensions were centrifuged at once 4000 rpm and once 10000 rpm and redispersed in distilled water. The white light emission SNPs were performance mixing the three molecules (BT3:ACN1:DBBT3-Hex) the ratios employed were 0.15:1:0.15 and 1.1:1.5:1.2 respectively.

4.4 Results and discussion

4.4.1 Characterization of molecules in solution and aqueous suspension of organic NPs and SNPs

Molecules were prepared by synthetic methodologies, and spectroscopic characterization by means of nuclear magnetic resonance (NMR) and IR spectroscopy techniques was carried out to establish the molecular structure. Already synthesized and characterized the molecules were prepared a solution (1×1^4 M) in THF from BT3, ACN1, BT2, BT20 and DBBT3-Hex molecules. UV-Vis absorption spectra of chromophore BT3, shows an intense band around 362 nm assigned to $\pi \rightarrow \pi^*$ electronic transition, due to molecular structure this molecule has poor intramolecular charge transfer character. However the benzothiadiazole derivative ACN1, BT2, BT20 and DBBT3-Hex, have a strong intramolecular charge transfer (ICT) transition toward the acceptor core. In this case the spectra shapes are observed with two absorption bands, one of them of greater intensity assigned to ($\pi \rightarrow \pi^*$) electronic transition at 272 nm for ACN1, 275 nm for BT2, 367 for BT20 and 332 nm for DBBT3-Hex and the other absorbance band corresponding to ICT is found at 382, 444, 502 and 495 nm respectively for ACN1, BT2, BT20 and DBBT3-Hex. These main electronics transitions are from peripheral aryl moieties (Donor) to central core (acceptor), which indicative of the quadrupole architecture (D-π-A-π-D). These chromophores in solution show a high photoluminescence emission in blue (BT3) at 390 nm, green

(ACN1 and BT2) at 494 nm and 523 nm and red (BT20 and DBBT3-Hex) at 622 nm and 628 nm, respectively. As a first approximation, the mathematical mixture of these emission in blue, green and red cover a broad spectrum from 390 to 800 nm (Fig 4.9), with the blends of fluorophores is possible to obtain white emission. The calculated Stokes shift for each fluorophore in solution was from 1980 to 17800 cm^{-1}. Normalized absorption and photoluminescence spectra of these molecules are presented in Fig. 4.2, the mixtures of these molecules are used to obtain RGB solutions with white-emission. This method to obtain white light is based on the blend of an excellent donor material (in this case BT3) with an amount of narrow band gap light-emitting molecules (here were used ACN1, BT2, BT20 and DBBT3-Hex), and then using the incomplete energy transfer (ET) to achieve white light emission [79]. In addition, from the absorption spectra is observable the possibility the excitation of all fluorophores with 375 nm. As a first approximation, for these fluorophores were calculated optical band gap from absorption bands, values obtained were of 3.43, 3.25, 2.80, 2.47 and 1.51 for BT3, ACN1, BT2, BT20 and DBBT3-Hex, respectively.

In order to determine the HOMO and LUMO energy levels of molecules and establish the correlation with observed optical properties, electrochemical cyclic voltammetry technique was carried out, Table 4.1 summarized the calculated values by cyclic voltammetry technique, optical techniques and theoretical methods. Geometrical optimization of structure for molecules BT3, ACN1, BT2, BT20 and DBBT3-Hex (for two monomers) were carried out by using DTT and DFT theoretical level in general, the molecules showed a semi-planar conformation. Molecular modeling was performed on the GAUSSIAN 09 program using the B3LYP functional. All structures were fully optimized in gas phase without any symmetrical restriction at 298.15 K. The HOMO-LUMO values were calculated theoretical and are plotted over molecular structure Fig. 4.3. Frontier Molecular Orbitals (FMOs) of the five derivatives are shown in the more stable molecular conformation. In particular, is denoted that theoretical calculations indicate an electronic transition from HOMO to LUMO promotes a quadrupole architecture D-A-D for BT3 and ACN1, BT2 and BT20 molecules. The electronic densities in HOMO levels are localized around all structure, contrary to what is observed in the LUMO levels where the electron den-

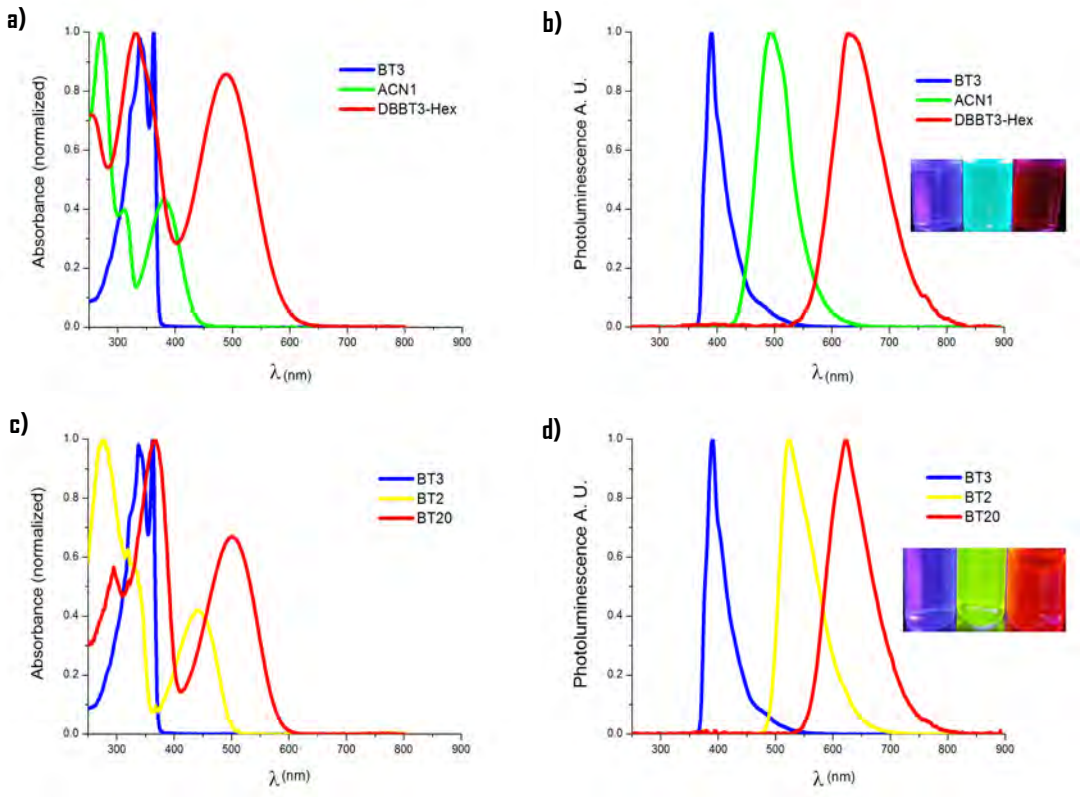

Figure 4.2: a), c) Normalized absorption. b), d) Normalized PL of the molecules in solution; The inset photography are corresponding at solutions under a UV excitation.

sity is located in the center of the molecule. In the LUMO energy level the electronic density for ACN1, BT2, BT20 and DBBT3-Hex is localized on the benzothiadiazole (BT) and in the central fluorene for BT3. These results corroborate the two-photon absorption (TPA) property which shows these three organic molecules [80].

The matching of the HOMO and LUMO energy levels of molecules as well as electrical and optical properties are important in the RGB mixtures in aggregation state, so that the energy transfer between them. Analysis of the experimental HOMO-LUMO levels indicates that the tendency on band gap is well reproduced by theoretical calculations with nevertheless a maximum deviation of 0.17 eV. For BT3 a high LUMO level and large band gap is required for intense absorption and

Table 4.1: Energy levels HOMO-LUMO en Energy Gap.

Compounds	Measured by CV HOMO $[eV]^a$	LUMO $[eV]^a$	$E_g[eV]^a$	Simulated HOMO $[eV]^b$	LUMO $[eV]^b$	$E_g[eV]^b$	$E_g[eV]^c$
BT3	-5.08	-1.62	3.46	-5.1	-1.7	3.4	3.43
ACN1	-5.77	-2.71	3.06	-5.9	-2.8	3.1	3.25
BT2	-5.27	-2.86	2.41	-5.2	-2.9	2.3	2.80
BT20	-4.95	-2.91	2.04	-4.9	-3.0	1.9	2.47
DBBT3-Hex	-4.69	-2.88	1.87	-4.8	-3.1	1.7	2.51

[a] *HOMO, LUMO energy levels and band gap were calculated from the cyclic voltammogram.*
[b] *HOMO, LUMO energy levels and band gap were simulated by theory calculations.*
[c] *Band gap measured optically, through UV-vis absorption spectra.*

emission, which is indicate the possibility to be a donor material.

Moreover, aqueous suspensions of NPs (with a concentration around 1×10^{-4}M) of fluorescent organic molecules BT3, ACN1, BT2, BT20 and DBBT3-hex were prepared by reprecipitation method using CTAB as a surfactant from THF solution at concentration 1×10^{-3} M. These suspensions were fabricated to ensure that the organic substances conserve fluorescent properties inclusive in a presence of biological medium such as saline solution. The aromatic molecules can lead to the formation of amorphous aggregates due to amorphous internal structure and their character hydrophobic π-conjugated. In most cases, the intermolecular $\pi-\pi$ stacking induces collisional interactions between molecules in the ground and excited states and subsequent fluorescence quenching are present in aggregated state [2, 14]. The emission bands for molecules BT3, BT2, BT20 and DBBT3-Hex is slightly red-shifted as a consequence of the $\pi-$ *stacking* involved in the chain collapse, unfortunately the quantum yield is lower ($\approx$ 50%) compare to the THF solution (100%). Although, in the case of ACN1 there is a blue-shifted might be due to the internal organization in the aggregate, and the quantum yield after aggregation is reduced at $\approx$ 86% compared to the THF solution (100%). Whereas for BT2 the emission of the aggregation is slightly red-shifted, and the quantum yield is about the same as the THF solution. In most cases the absorption spectra of the nanoparticles shows red-shifted

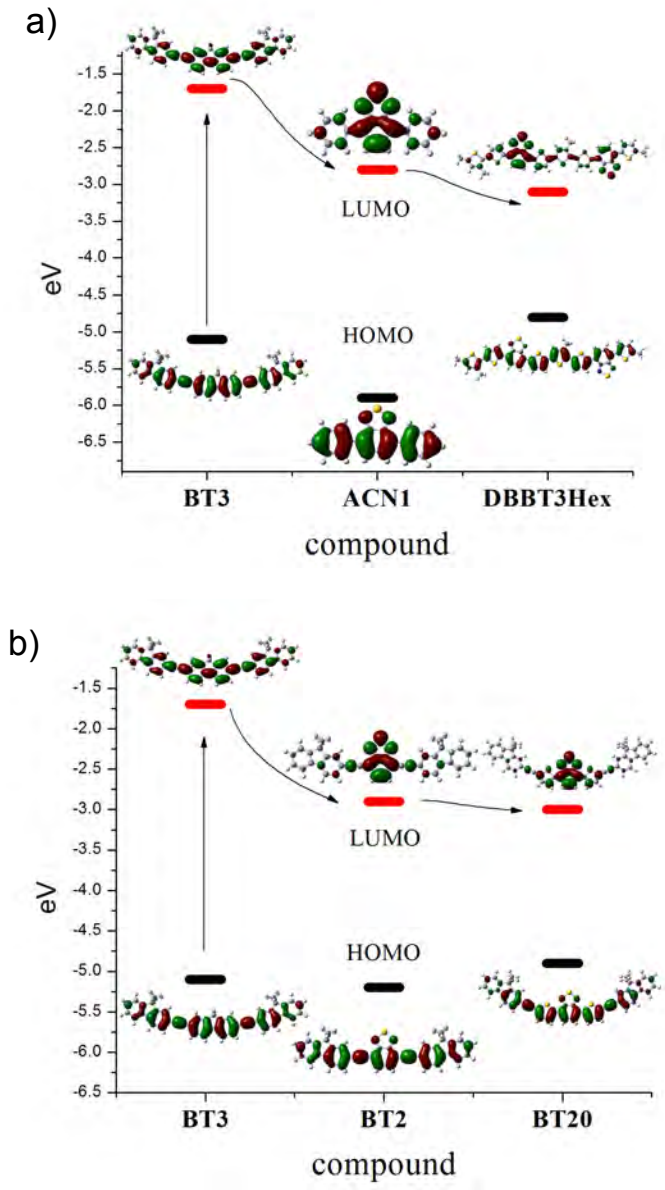

Figure 4.3: Gas-phase orbital pictures for the five molecules BT3, ACN1, BT2, BT20 and DBBT3-Hex for two monomers. HOMO/LUMO undergo a redistribution of electronic density from the entire frame to only the acceptor core center (D-A-D; quadrupole architecture); a) RGB1-BT3:ACN1:DBBT3-Hex and b) RGBBTs-BT3:BT2:BT20.

in comparison to the molecule dissolved in a good solvent. There are some reports that show an increase in the conjugated length of the molecular backbone by inter-

molecular interactions [17, 19, 31, 81, 82]. Optical properties of suspensions were evaluated by absorption and PL spectra and are present in Fig. 4.4 and Fig. 4.5. These spectroscopic data were taken as a first indication of the formation of NPs from solutions of materials.

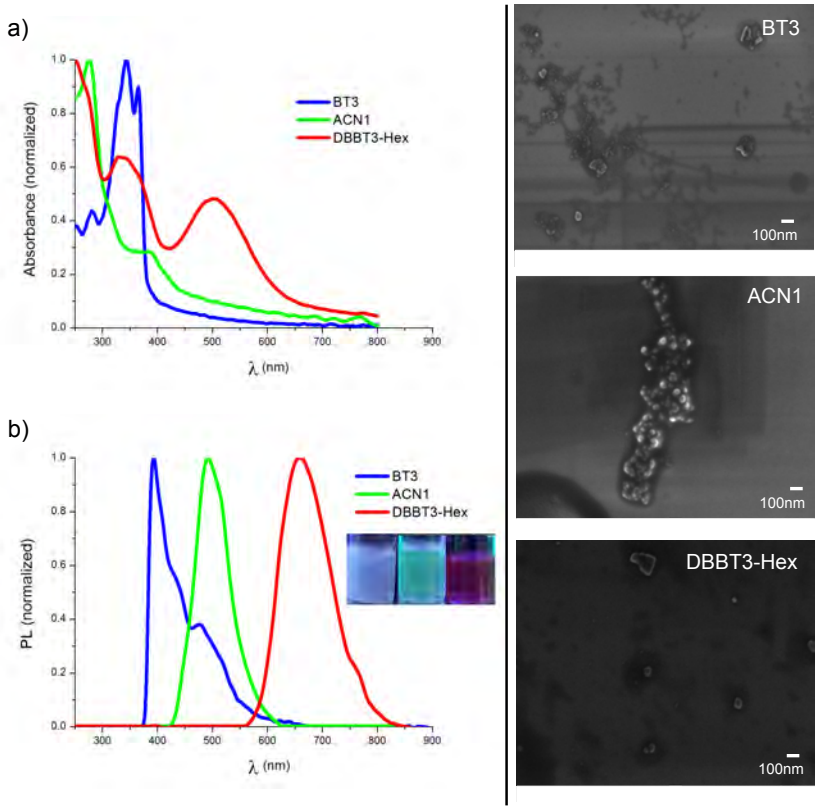

Figure 4.4: a) Normalized absorption. b) Normalized PL of the molecules in aqueous suspension for BT3:ACN1:DBBT3-Hex (RGB1). The inset photography are corresponding at solutions under UV excitation. On the right, SEM micrographics of NPs fabricated by reprecipitation.

The emission spectra of the aqueous suspension fabricated by reprecipitation shows that the photoluminescence properties are conserved from solution to suspension, the CIE color coordinates were calculated in data are summarized in Table 4.3. Analysis of the morphologies for NPs were carried out by scanning electronic microscopy (SEM), the results indicate that NPs obtained have amorphous morphology (irregular shapes), on the right of Fig. 4.4 and Fig. 4.5, are showed the SEM

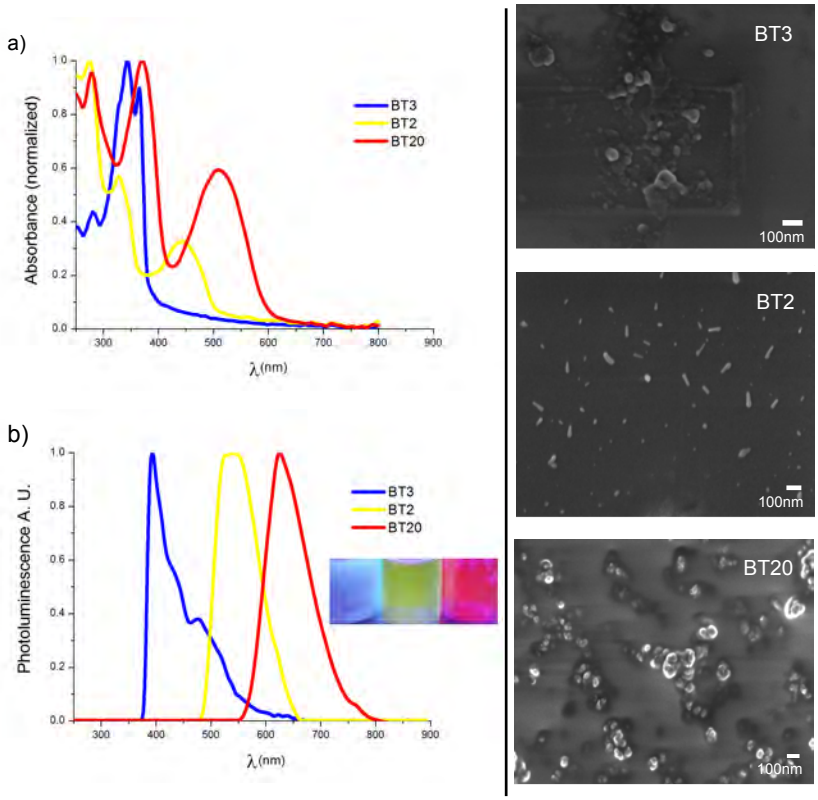

Figure 4.5: a) Normalized absorption. b) Normalized PL of the molecules in aqueous suspension for BT3:BT2:BT20 (RGBBTs). The inset photography are corresponding at solutions under UV excitation. On the right, SEM micrographics of NPs fabricated by reprecipitation.

images of the NPs. Furthermore, from the images obtained by SEM microscopy were calculated the size distributions of NPs employing image J software and compared with those measured by DLS technique. The hydrodynamic diameter measured by DLS are 189.8±97.18 nm for BT3, 159.2±39.38 nm for ACN1, 241.3±113.7 nm for BT2, 305.4±127.0 nm for BT20 and 198.7±91.91 nm for DBBT3-Hex, analysis of size dispersion of the NPs fabricated by reprecipitation technique shows a standard deviation and high polydispersity (this index provides information on the sample values close to 0 indicate that the sample is monodisperse and values close to unity indicate that the sample has a wide variety of sizes). Size distributions by SEM technique for five molecules were less (average diameters between 20-80 nm), this disagreement is may be due to by DLS is measured the hydrodynamic diameters of

nanoparticles and the samples are evaluated dry and are not hydrated, (Table 4.2). In a) Fig. B.5 is shows the size distributions measured by DLS technique.

Table 4.2: Size of nanoparticles by reprecipitation (NPs) and microemulsion (SNP), measured by SEM microscopy and DLS technique.

Sample	D_{SEM} (nm)	D_{DLS} (nm)	Pdl_{DLS}
$BT3_{NPs}$	$26-50^a$	189.8±97.18	0.185
$BT3_{SNPs}$	44	106.0±42.95	0.265
$ACN1_{NPs}$	$24-50^a$	159.2±39.38	0.347
$ACN1_{SNPs}$	48	79.36±25.27	0.159
$BT2_{NPs}$	$14-80$	241.3±113.7	0.215
$BT2_{SNPs}$	56	88.55±24.68	0.077
$BT20_{NPs}$	$38-80$	305.4±127.0	0.198
$BT20_{SNPs}$	46	176.2±89.89	0.196
$DBBT3-Hex_{NPs}$	$24-52^a$	198.7±91.91	0.200
$DBBT3-Hex_{SNPs}$	50	212.6±116.0	0.219

[a] *interval size distribution.*

Unfortunately, the compounds BT3 in aqueous suspension is unstable, there are some reports about degradation of fluorene moiety. Yuguang Ma et. al [83], photodegradation of fluorene oligomers that poses alkyl and aromatic substitutions in the bridged C-9 position under UV-light irradiation. Results indicate that the formation of ketonic defects after degradation depends on the proportion of alkyl substitution. Marian Asantewah Nkansah et. al [84] investigate the direct photochemical degradation of aqueous fluorene solution under UV-light irradiation, they found that formation of among of hydroxyl radicals which are involved in the oxidation of fluorene fluorophore. The possible initial oxidation chemical reaction of fluorene derivate with hydroxyl radicals is expected to give rise to 9H-fluorene-9-one compound.

In this way to increase the stability of fluorophores in aqueous suspension were fabricated nanoparticles coated with silica (SNPs), which provide a protective layer, thereby reducing photo-oxidation of the molecules. Photophysical properties of SNPs based on BT3, ACN1, BT2, BT20 and DBBT3-hex fluorophores were investigate and are summarized on Table 4.3. On the right in Fig. 4.6 and Fig. 4.7 are showed the

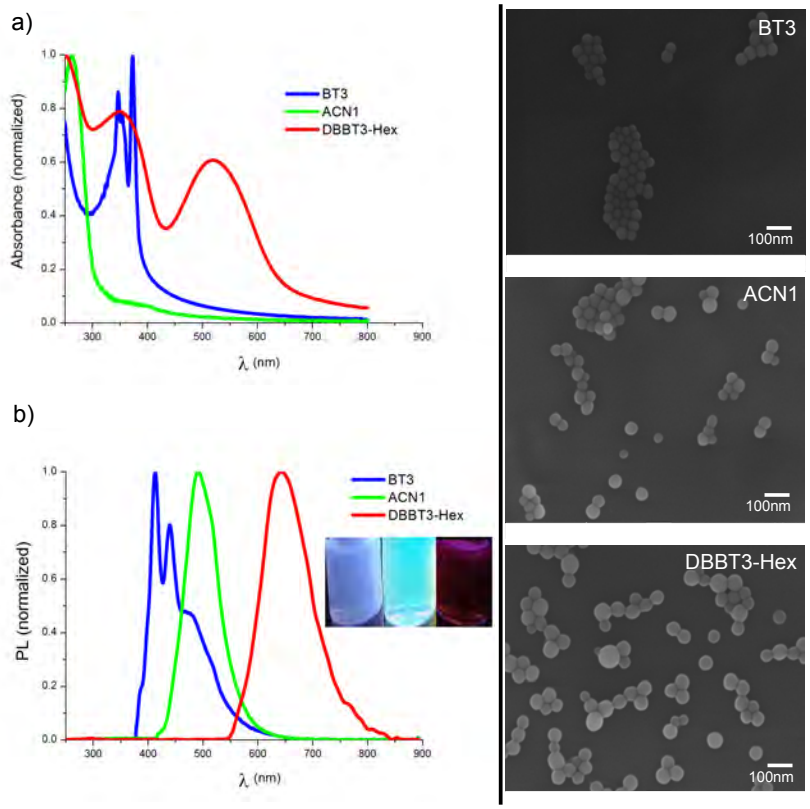

Figure 4.6: a) Normalized absorption. b) Normalized PL of the SNPs for BT3:ACN1:DBBT3-Hex (RGB1). The inset photography are corresponding at solutions under UV excitation. On the right, SEM micrographics of SNPs fabricated by microemulsion.

SEM images to SNPs, their morphology shown are typically spherical. For analysis of distribution size of NPs were used these micrographics, the size measured is about 44-50 nm. Moreover, DLS measurement shows the polydispersity data in average of 0.183 which are lower than obtained for NPs fabricated by reprecipitation method, those results of the DLS measurements for SNPs are shown in Fig. B.5. A summarized data obtained for organic fluorophores in solution, aqueous suspension and SNPs are showed into Table 4.3. The photoluminiscence emission wavelength for fluorophores in solution compared with NPs or SNPs present a bathochromic shift of 23 nm for BT3, 25 nm for BT2, 16 nm for BT20 and 30 nm for DBBT3-Hex molecules, is observed an exception for ACN1 in which a hypsochromic shift was observed of 4 nm. These changes showed for emission bands are directly observed in

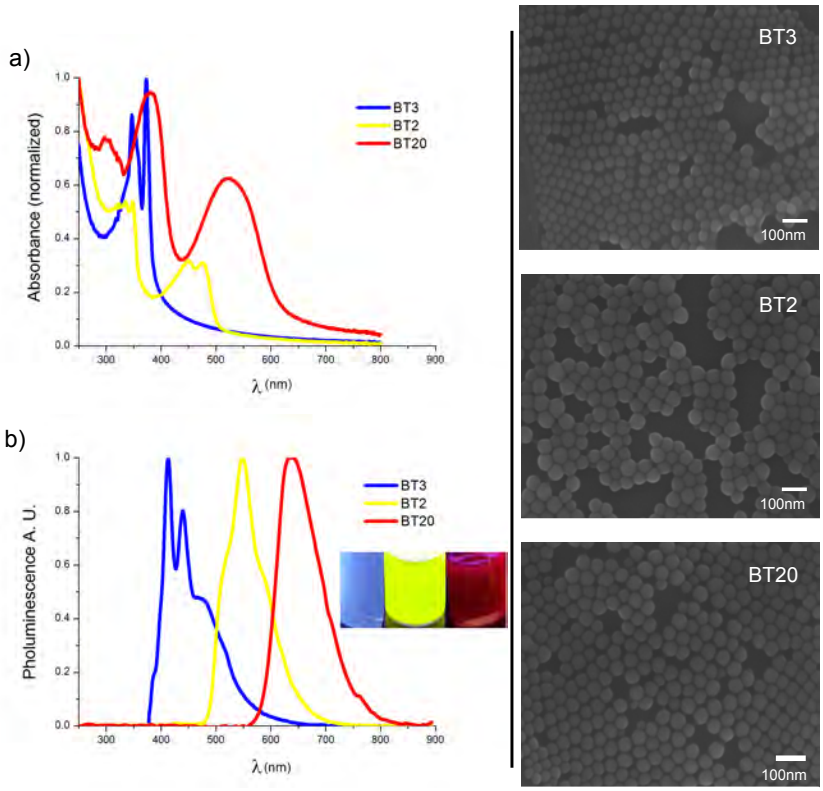

Figure 4.7: a) Normalized absorption. b) Normalized PL of the SNPs for BT3:BT2:BT20 (RGBBTs). The inset photography are corresponding at solutions under UV excitation. On the right, SEM micrographics of SNPs fabricated by microemulsion.

the calculated color coordinates by using CIE 1931 method (Fig. 4.8). It is important to note that SNPs exhibit a significant quenching of the quantum yield for the five molecules compared with corresponding solutions or inclusive to NPs formed by reprecipitacion, this behavior could be attributed to silica coating.

For those emission spectra with color coordinates in region of the equal energy point (0.33, 0.33), can be called white light according to CIE 1931 [79]. According to color theory, all the color spectra can be achieved by mixing the three primary colors, so white light can also be obtained in this way. In general, each color have a coordinate then link lines of color coordinates of three of them constitute one triangle. As long as the triangle contains equal energy point, the white color can be

Table 4.3: Photophysical parameters and color coordinates (xy) of five molecules.

Compounds	λ_{abs} (nm)	λ_{em} (nm)	Stokes shift (cm^{-1})	ϕ	Color coordinates (x, y)
$BT3_{THF}$	362	390	1980	0.23	0.15, 0.06
$BT3_{NPs}$	342	393	3620	0.15	0.16, 0.17
$BT3_{SNPs}$	373	413	2600	0.05	0.16, 0.16
$ACN1_{THF}$	272	494	16500	0.72	0.17, 0.43
$ACN1_{NPs}$	276	491	15900	0.10	0.17, 0.42
$ACN1_{SNPs}$	263	490	17600	0.13	0.17, 0.40
$BT2_{THF}$	275	523	17200	0.87	0.35,0.62
$BT2_{NPs}$	275	539	17800	0.83	0.38,0.59
$BT2_{SNPs}$	348	548	10599	0.15	0.40,0.57
$BT20_{THF}$	367	622	11200	0.46	0.63,0.37
$BT20_{NPs}$	370	625	11000	0.24	0.65,0.35
$BT20_{SNPs}$	380	638	10600	0.05	0.67,0.33
$DBBT3-hex_{THF}$	332	628	14200	0.20	0.63, 0.36
$DBBT3-hex_{NPs}$	331	658	15000	0.17	0.67, 0.33
$DBBT3-hex_{SNPs}$	350	643	13000	0.02	0.64, 0.35

achieved, of course the proportion will be adjusted [79]. The (x, y) values calculated for the five chromophores of this thesis are between red, yellow, green and blue color, and from combinations is accessible a broad range of colors (gamut). By using the principle of mixing these compounds in correct proportions we can obtain white-light emission, reproducing color in a molecular scale by simple mixing of different RGB chromophores due to the inherent energy transfer between them.

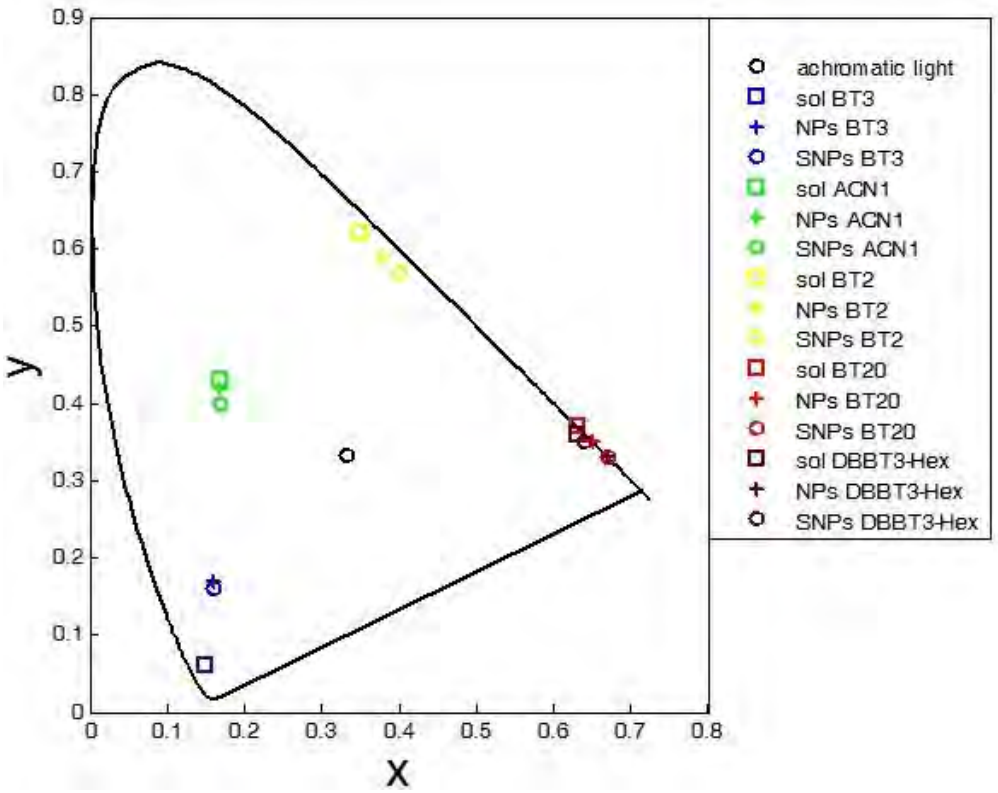

Figure 4.8: CIE color coordinates diagram of the molecules in solution, NPs and SNPs.

4.4.2 White light emission of RGB mixtures in solution and nanoaggregation

By using the principle of RGB mixtures the white light is made from the sum of emission band in regions of the visible spectrum. The methods for producing white light, can be classified according to the number of color molecules employed. It is possible produce white light by mixing the three ”primary colors” i.e. by mixing red, green and blue fluorescent materials, another approach is by using “complementary colors” where the combination of only two colors can produce white light for example the combination of yellow and blue colors [32]. The two complementary color mixing method has the advantage of easy control of the CIE (x, y) color coordinates, in contrast, on three primary color mixing method the control is more complicated. The interest to obtaining white light in science and technology has increased due

to the application of these materials as WOLED's and biomedical markers. Currently, the most popular organic emitters are small molecule and exists a grand variety of them such as carbazolyl, fluorene, benzothiadiazole derivatives [64]. The emission of these molecules (or dyes), is often weakened or quenching after to fabricate nanoaggregates, this phenomena is known as aggregation caused quenching (ACQ) [24]. ACQ phenomenon is even more serious for molecules with emission in the far-red/near-infrared (FR/NIR) which are interesting for having emission in the tissue-transparency window. In addition, some molecules in which elongated $\pi - conjugation$ is promoted by using aromatic rings the photoluminescence property is reduced due to strong π–π interaction that are responsible to quench the fluorescence.

To investigate the possibility of fabricating RGB mixtures based on fluorophores RGB1- BT3:ACN1:DBBT3-Hex and RGBBTs-BT3:BT2:BT20, as a first approximation were combined mathematically their emission spectra in solution, NPs and SNPs. The corresponding graph to the sum of the emission spectra for possible combinations are showed in Fig. 4.9, to obtain these curves were considered the quantum yields of each molecule on the environment in which they were found and also the proportions of fluorophore used in the mixtures. However, in these graphs was not considered the phenomena of energy transfer (eg Dexter or Förster Energy transfer, radiative transfer) between organic molecules involved. Moreover, this approximation indicates that a possible white light-emission is achieved from combination of BT3:ACN1:DBBT3-hex and RGBBTs-BT3:BT2:BT20 derivatives.

Fig. 4.9 shows the spectrum of white light emission, due to the summation of the emission bands corresponding to the fluorophores in solution (a-b), SNPs (c-d) and SNPs (e). The analysis of RGB1 spectra mixtures denotes that the most intense band is around 500 nm, which corresponds to the emission of ACN1 molecule, in comparison for mixture of NPs emission bands the maximum intensity emission correspond to the band of the BT3 compound (around 400 nm). Is worthy to mention that the emission band with lower intensity in all the summations correspond to the molecule with emission in red color, which is DBBT3-Hex and BT20 on RGB1 and

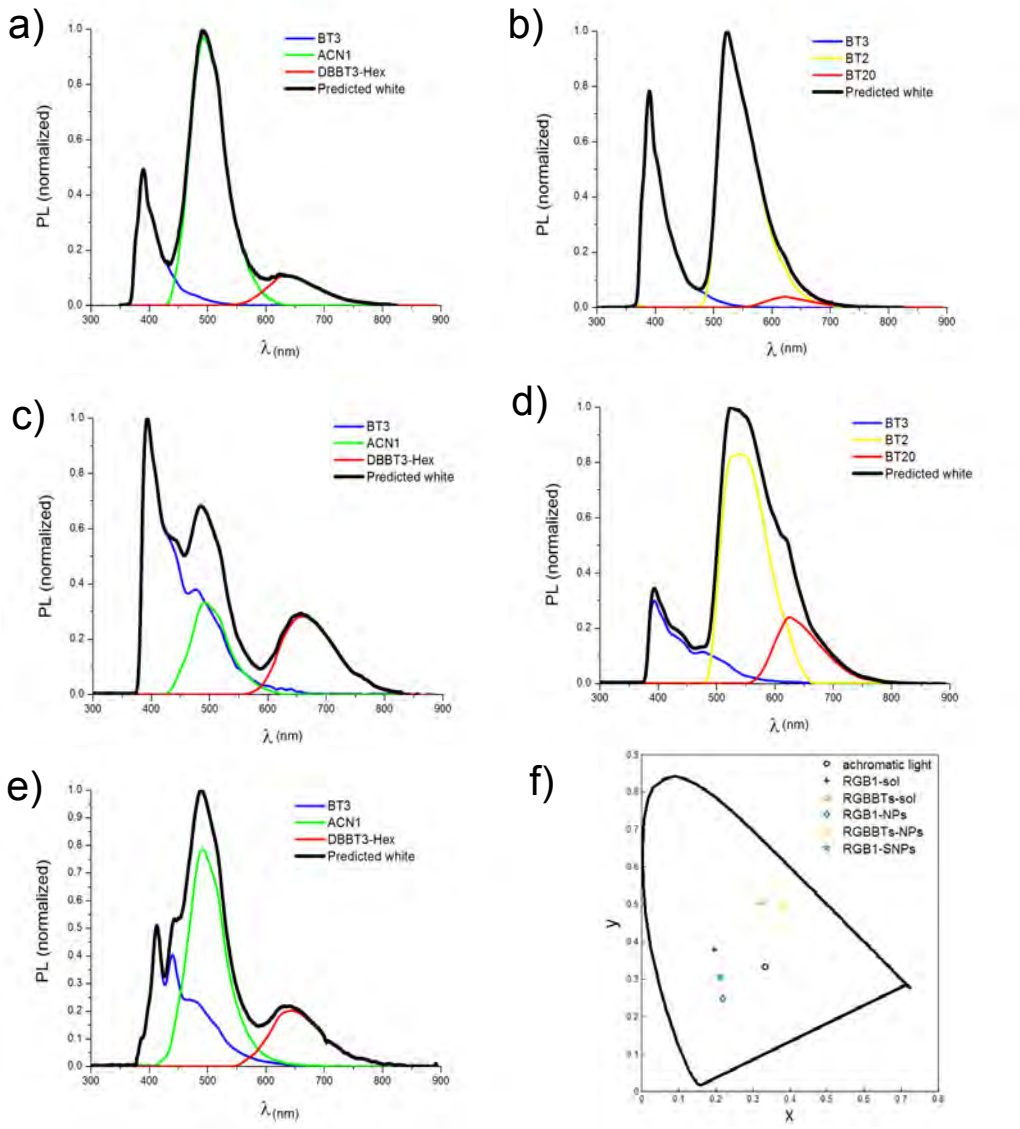

Figure 4.9: Prediction of white light emission derived from the sum of emissions for the two triads: BT3:ACN1:DBBT3-Hex and BT3:BT2:BT20 in a) and b) solution; c and d) NPs and e) SNPs and f) The diagram of the color coordinates.

RGBBTs mixtures, respectively. In order to achieve solutions showing white light emission, a mixture was prepared from the three organic molecules with blue, green and red emission color. After to investigate mixtures with different ratios of fluorophores, a THF solution with white light emission was obtained for combination of

DBBT3-hex:ACN1:BT3 in a molar ratio of 0.5:1.5:2 (Fig. 4.10). While, for RGBBTs solution the mixture with similar emission was fabricated by using BT20:BT2:BT3 in ratio of 0.5:7:20 (Fig. 4.11). These emission spectra were obtained by using 375 nm as excitation source, to verify its emission in white the color coordinates were calculated from emission spectra and the data are summarized on Table 4.4. To compare the calculated with experimental spectra, we observed that in both mixtures BT3 compound is present in highest proportion, however, its emission band is not the most intense, this suggests that there a possible energy transfer process is happening. This electronic phenomenon could be due to different mechanism as multiple excitation energy transfer (EET), through FRET or trivial mechanisms, in all previous cases the resulting is the enhanced emission from the red-emitting fluorescent units which acts as the energy acceptors.

The electrical and optical properties of the WOLED depends on the energy transfer between the host (donor) and dopants (acceptors) and it is affected by the energy band gap of the component [85, 86]. On the basis of these considerations, EET should increase with smaller energy gaps between the LUMO energy levels of donor and acceptor components [85], To analyze this for chromophores used in this work, the HOMO-LUMO energy band diagram was develop and is shown in Fig. 4.3. From this figure is possible to predict the energy transfer process between the components of the mixture. According to this assumption, a possible energy transfer process occurs from BT3 fluorophore to ACN1 chromophore and from ACN1 to DBBT3-Hex at the RGB1 mixture, experimentally was evaluated this energy transfer between ACN1 and DBBT3-Hex in suspension, are showed in Fig. B.4. For the RGBBTs mixture, the ET is possible to happen from BT3 to BT2 and from BT2 to BT20, this due to the degree of overlap between the absorption and PL emission peaks of the materials that are show in Fig. B.4 and Fig. B.3.

Absorption and emission spectra of the suspensions are show in Fig. 4.10 and Fig. 4.11, the CIE coordinates are found in Table 4.4. The energy transfer evaluation was only made for ACN1 and DBBT3-Hex in suspension (NPs), the study is show in Fig. B.4. Fig. 4.10 morphological analysis of the NPs was develop by using

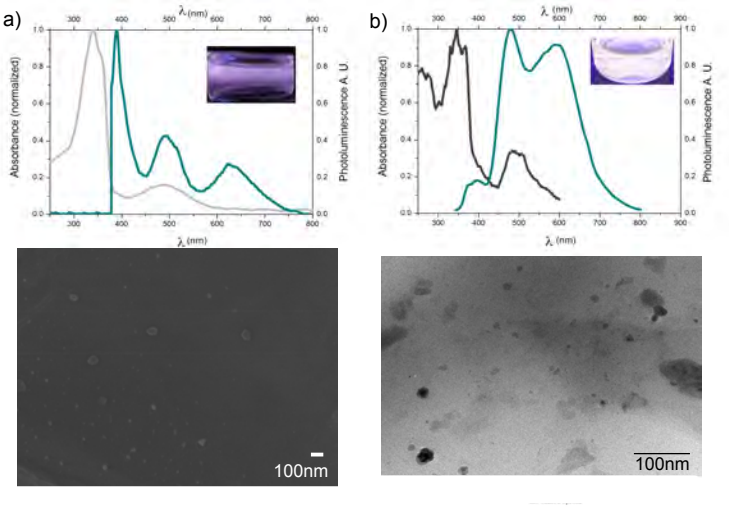

Figure 4.10: Normlized absorption and emission spectra for a) RBG solution; b) RGB suspension. The emission spectra are recorded at 375nm and 343nm respectively, the inset photography are corresponding at suspension under UV excitation. On the bottom, are showed the SEM and TEM images of the NPs.

SEM and TEM techniques, results showed for RGB1 NPs with small size, commonly not so large than 50 nm, again the result is not consistent with those obtained by DLS technique, see Table 4.2. The size distribution obtained from DLS is shown in Fig. B.7. Fig. 4.11 shows the SEM images for RGBBTs and RGBBTs NPs. By comparing the SEM images and DLS measurements of the two suspensions (RGB1 and RGBBTs) is observed that the sizes of the nanoparticles RGBBTs are larger than RGB1 NPs.

Fluorescent silica nanoparticles with multiple emission wavelengths by single wavelength excitation have been studied for multiplex bioanalysis in recent years. These multicolor silica nanoparticles can be used as barcoding tags for multiplexed signaling [22]. For the SNPs fabricated from fluorophores used in this work was evaluated their optical properties and then were prepared suspension with white light emission by mixing the SNPs of each molecule (Fig. 4.12). Absorption and emission spectra of suspensions were acquired, the proportions used of R:G:B SNPs were 1:2:0.5, and its color coordinates were x=0.30, y=0.35, which is closer to the desired pure white region. Comparing the predicted emission spectra shown in Fig.4.9

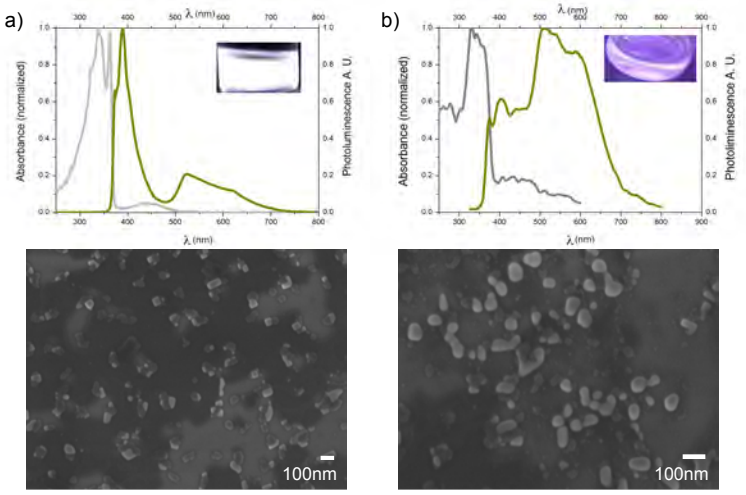

Figure 4.11: Normalized absorption and emission spectra of RGBBTs at a) RBG solution; b) RGB suspension (NPs). The emission spectra are recorded at 375, 325nm, the inset photography are corresponding at suspension under UV excitation. On the bottom, are showed the SEM images of the NPs.

and obtained experimentally is observed that the emission peak corresponding to DBBT3-Hex molecule is more intense in the spectrum obtained experimentally than the calculated. In the mixture for obtain white-light emission, the amount of DBBT3-Hex was smaller than those used for ACN1, an explanation for why a large amount of ACN1 is required in compared to DBBT3-Hex, is due to the overlap of the emission band of ACN1 and the absorption band of DBBT3-Hex (Fig. B.4), the green emission from ACN1 (donor) is reabsorbed by DBBT3-Hex (acceptor). The green and red emitters are in close enough proximity, energy transfer occurs from donor to acceptor molecule and photoluminescence is obtained. The remaining green emission which are not involved in energy transfer is used to complete the white emission spectra.

In Fig. 4.12 shows the absorption, emision and SEM micrography of the SNPs, their color coordinates were 0.21,0.35 and 0.43,0.38. In Fig. B.7 shows the size distributions measured by DLS technique.

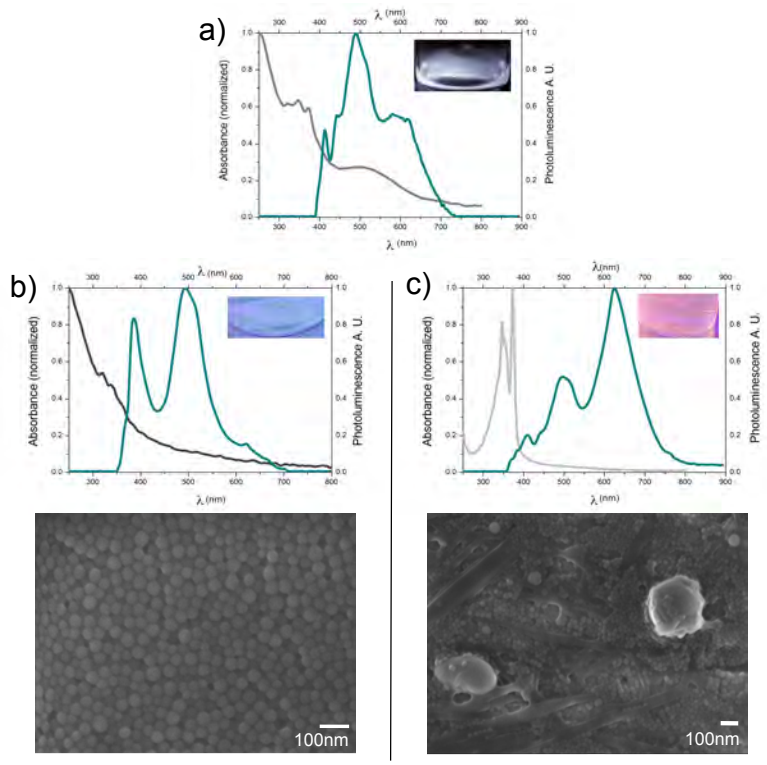

Figure 4.12: Normalized absorption and emission spectra of RGB1SNPs: a) separately mixing the SNPs of each molecule; SNP samples with different molecules combinations; b) and c) RGB SNPs at different ratios. The inset photography are corresponding at SNPs under UV excitation. On the bottom, are showed the SEM images of the SNPs.

Comparison of the mixtures RGB mixtures in solution, NPs and SNPs

In solution obtaining the white emission was easier because the distance between molecules is higher than in aggregate so that the energy transfer is minimal, so in the case of solution RGBBTs its color coordinates are very close to the region of pure white. Afterwards, to obtain the white-light nanomaterials by reprecipitation method was affected by several factors such as the order in which the molecules were adding and the change of the ratios doe to energy transfer between molecules. From the emission spectrum of RGB1 and RGBBTs NPs the color coordinates were calculated to corroborate the white light emission, these fall in the white region and the nanoparticles size distribution is acceptable around 128.9±49.55. While, by

microemulsion method white-emission nanomaterials showed greater stability doe to silica coating, so the photodegradation of BT3 was greatly reduced. All values are shown in the following Table 4.2.

Table 4.4: Size of RGB nanoparticles by reprecipitation (NPs) and microemulsion (SNP), measured by SEM microscopy and DLS technique.

Sample	CIE coordinates (x, y)	D^{a}_{SEM} (nm)	D_{DLS} (nm)	Pdl_{DLS}
$RGB1_{THF}$	0.29,0.30	-	-	-
$RGBBTs_{THF}$	0.31,0.33	-	-	-
$RGB1_{NPs}$	0.35,0.38	$16-40$	137.0±56.32	0.183
$RGBBTs_{NPs}$	0.34,0.39	$38-92$	128.9±49.55	0.121
$RGB1-1_{SNPs}$	0.21,0.35	15-50	40.37±19.58	0.305
$RGB1-2_{SNPs}$	0.43,0.38	15-75	278.5±152.7	0.463

[a] *Interval size distribution. And color coordinates (x,y), of RGB solution, NPs and SNPs.*

Chapter 5

Conclusions

The purpose of this thesis was the study of the photoluminescent properties of five organic molecules (BT3, ACN1, BT2, BT20 and DBBT3-Hex) in solution and nanoparticles, these organic molecules proved to be highly and moderately fluorescent in solution of organic solvent and aqueous suspension, respectively. Fluorescence quenching after the formation of amorphous aggregates is probably due to amorphous internal structure and their hydrophobic character. The compound having greater photoluminescence in both solution and aggregate state was BT2, while less photoluminescent emission is showed for DBBT3-Hex compound. Nanoparticles fabrication was carried out by two methods: reprecipitation (NPs), and microemulsion (SNPs) methods for these nanomaterials their sizes and morphologies were established by DLS and SEM experiment. Reprecipitation method has some advantages such as: quick and easy preparation, but in the other hand, makes difficult to precisely control the nucleation process and growth, thus NPs morphological analysis of BT3, ACN1, BT2, BT20 and DBBT3-Hex fluorophores showed variations in sizes from 14 nm to 80 nm and the irregular shapes. In comparison by microemulsion method, nanoparticles were coated with silica, for this method was obtained sizes distribution lower than reprecipitation method and morphology observed was regular spherical shape.

Photophysical characterization of chromophores was developed in solution and aqueous suspension, for compound BT3 in aqueous suspension was observed that is unstable. Photodegradation of fluorene moety has been previously studied and is

attributed to the oxidation reaction of C-9 owing to UV illumination. Then, after BT3 derivative was coated with silica its stability increase approximately 60%, the study is present in Appendix B Fig. B.2.

Finally, the specific focus of this thesis is the fabrication of nanomaterials with white light-emission by combination of three three "primary colors" red, green and blue materials. For this work, we employ two different triads: RGB1-DBBT3-Hex:ACN1:BT3 and RGBBTs-BT20:BT2:BT3. In solution the two triads present a white light emission which is corroborate by color coordinates, important to note that for RGBBTs was almost obtained a perfect white color. Moreover, by reprecipitation method also was obtained aqueous suspension of nanomaterials with white emission. By the microemulsion method were obtained the nanomaterials with silica coating, which protects the organic molecules, presenting greater stability mainly for BT3 compound which it is unstable in aqueous suspension. Photophysical study of these with light-emitter showed an energy transfer between the molecules by way of RET or/and FRET process. The existence of ET in nanoclusters generates a large Stokes shift favoring its application as biological labeling and imaging. For the development of WOLEDs the electrical and optical properties depends on the energy transfer, so is important energy transfer existence between the host and dopants.

Appendix A

Suplementary theory information

A.1 Colorimetry

In this apendice is intended to give a brief explanation of how we perceive color and understand how the system of color measurement (tristimulus values, (XYZ), chomaticity coordinates (xy) and chromaticity diagram) is performed.

A.1.1 Measurement system CIE 1931

The CIE is an international organization which is concerned with everything related to color and color measurement, CIE for its French name Commission Internationale de l'Éclairage. With the aim of developing a color standard CIE conducted numerous experiments, the experiments were made in 1931 where at last a color matching system based on the experimental results obtained by Guild and Wright was adopted.

The CIE standard is based on three imaginary primaries that can be mixed by adding and form any color. For Standard 1931 primary agreement was picked as computational limitations of the time, deciding that the XYZ values must always give positive values for any stimulus actual color.

Tristimulus values (XYZ), chromaticity coordinates (x, y) and chromaticity diagram

Tristimulus values defined the amount of the set of primary and are used to find the color coordinates for a given stimulus. The bar on each variable indicates which is the average value, such $\bar{x}$ [87].

The magnitudes of the XYZ components are proportional to the radiometric power, but its spectral composition corresponds to characteristics of color similar to the human eye [61]. The graph of these functions are shown in a) Fig. A.1.

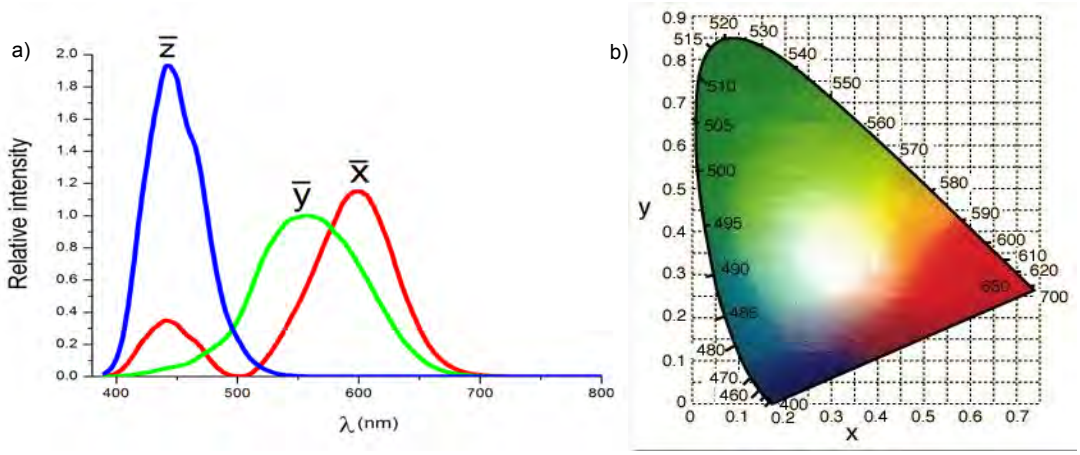

Figure A.1: a) Color match functions $\bar{x}_\lambda$, $\bar{y}_\lambda$ and $\bar{z}_\lambda$,of CIE 1931 b) Color diagram.

The concept of tristimulus values is based on the theory of the three color components which states that the human eye has recipients of the three primary colors: red, blue and green; and all the colors are mixtures derived from them. The XYZ tristimulus are calculated with the color functions $\bar{x}_\lambda$, $\bar{y}_\lambda$ and $\bar{z}_\lambda$ from standard observer using the equations [87]:

$$
\begin{aligned}
X &= k \sum_{390}^{830} \phi(\lambda)\bar{x}(\lambda)\Delta\lambda \\
Y &= k \sum_{390}^{830} \phi(\lambda)\bar{y}(\lambda)\Delta\lambda \\
Z &= k \sum_{390}^{830} \phi(\lambda)\bar{z}(\lambda)\Delta\lambda \\
k &= \frac{100}{\sum_{390}^{830} \phi(\lambda)\bar{y}(\lambda)\Delta\lambda}
\end{aligned}
\tag{A.1}
$$

Where $\phi(\lambda)$ is the spectral distribution of the source to be measured, $\bar{x}(\lambda)$, $\bar{y}(\lambda)$, $\bar{z}(\lambda)$ are the color match functions and $\Delta\lambda$ equal to 1nm, CIE 1931, defined by the observer pattern for each of the visible wavelengths and k is the relative luminance of the source and directly indicates the value of Y, given a value of Y equal for an absolute blank and a value equal to hundred for a perfect white, that defines the constant.

For the determination of the chromaticity coordinates must equations:

$$
\begin{aligned}
x &= \frac{X}{X+Y+Z} \\
y &= \frac{Y}{X+Y+Z} \\
z &= \frac{Z}{X+Y+Z}
\end{aligned}
$$

Any set XYZ can be represented in a chromaticity diagram. Even if only two of the three need be given, since $x + y + z = 1.00$. With beams of light of equal luminous intensity Y, the one with the highest value of y, also called the *luminance*, is perceived as being brightest. Thus the greens and yellows of b) Fig. A.1 have a higher luminance than blues and reds [88].

A.2 Energy transfer

A.2.1 Photoinduced Electron Transfer (PIET)

In organic systems, electron transfer to occur, the donor and acceptor should be sufficiently close that their molecular orbitals become overlapped. In quantum mechanics theory, this corresponds to a spatial overlap of the donor and acceptor wavefunc-

tions. Long-range electron transfer may take place when the donor and acceptor are linked through a bridge molecule. Therefore the PIET might be between two molecules (intermolecular), or between two moieties of the same molecule. In such process, the molecule or moiety providing an electron is called the donor (D), while the other molecule/moiety receiving the electron is called the acceptor (A) [89].

The complex [$D\bullet + A\bullet -$] is generally termed a charge-transfer (CT) state. When the donor and the acceptor are in the same molecule, this is termed an intramolecular charge-transfer (ICT) state. This CT state possesses a larger dipole moment as a result of charge separation and emits at a longer wavelength with a broad, structureless emission band. Thus, it generally becomes more stable in a polar medium, and its emission becomes remarkably red-shifted with increasing solvent polarity [89].

A.2.2 Excitation Energy Transfer (EET)

An excited molecule/chromophore (D) can transfer the excitation energy to another molecule/chromophore (A) under certain circumstances. The donor molecules typically emit at shorter wavelengths that overlap with the absorption spectrum of the acceptor [90, 91], Fig. A.2.

In the general case, D^* and A^* are both singlet electronic excited states (S_1), a case that is often termed as singlet–singlet energy transfer. There are other possibilities, such as triplet–singlet energy transfer (transfer of excitation from an excited donor in triplet state to produce an excited acceptor in singlet state), and triplet–triplet energy transfer [91], this energy transfer can be through radiative and no-radiative processes, which are explained below. Energy transfer processes occur typically on time scales that range from picoseconds to nanoseconds for singlet energy transfer up to milliseconds and seconds for triplet energy transfer, because of the much longer lifetimes of triplet states [91].

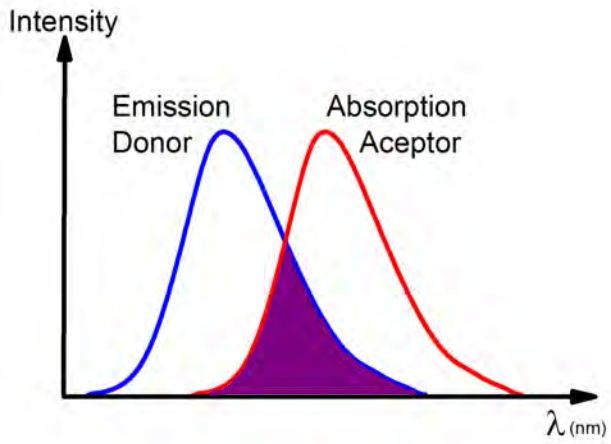

Figure A.2: Spectral overlap of the donor and acceptor required for EET.

Radiative energy transfer

This process is often called trivial transfer because of the simplicity of the phenomenon, but in reality the quantitative description is quite complicated because it depends on the size of the sample and its configuration with respect to excitation and observation. Radiative transfer results in a decrease of the donor fluorescence intensity in the region of spectral overlap. Such a distortion of the fluorescence spectrum is called the inner filter effect [92]. Upon photon emission the excited donor D^* returns to its ground state D while the ground state acceptor A will be promoted to its excited state A^* by the absorption process.

The efficiency of this process depends on the following four parameters: a) the quantum yield ϕ^D of D^* for emitting a photon, b) the number density n_A of ground state A molecules that can absorb the emitted photon, c) the absorption cross section $\sigma_A(\lambda)$, d) the overlap of the fluorescence emission spectrum of D^* and the absorption (or excitation) spectrum of A.

Non radiative energy transfer

Non-radiative transfer of excitation energy requires some interaction between a donor molecule and an acceptor molecule, and it can occur if the emission spectrum of the donor overlaps the absorption spectrum of the acceptor, so that several vibronic transitions in the donor have practically the same energy as the corresponding transitions in the acceptor. Moreover energy transfer can result from different interaction mechanisms: a) by collision, ei by intermolecular orbital overlap (Dexter energy transfer) and b) by Coulomb interaction, via dipole-dipole interaction (Förster energy transfer) [92].

For Dexter energy transfer the involved electronic orbitals collide and the excited donor electron is exchanged with an acceptor electron. The Dexter mechanism requires very small donor-acceptor distances with an interpenetration of their orbitals, the distances are around r $<$ 10 Å [90]. In contrast, the Förster mechanism occurs for larger distances over up to 10 nm. The Förster energy transfer involves a dipole–dipole coupling of the transition dipole moments for excited donor and the aceptor in its ground state. As the excited donor relaxes, its energy is transferred via a strong columbic interaction with the aceptor molecule [90].

Appendix B

Supporting information

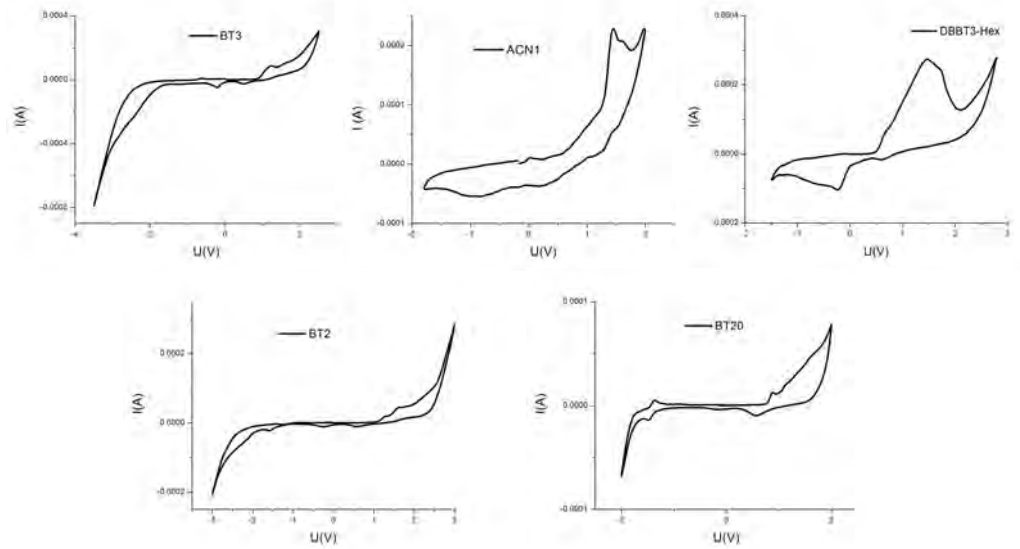

Figure B.1: Cyclic voltammetry curve for the five molecules.

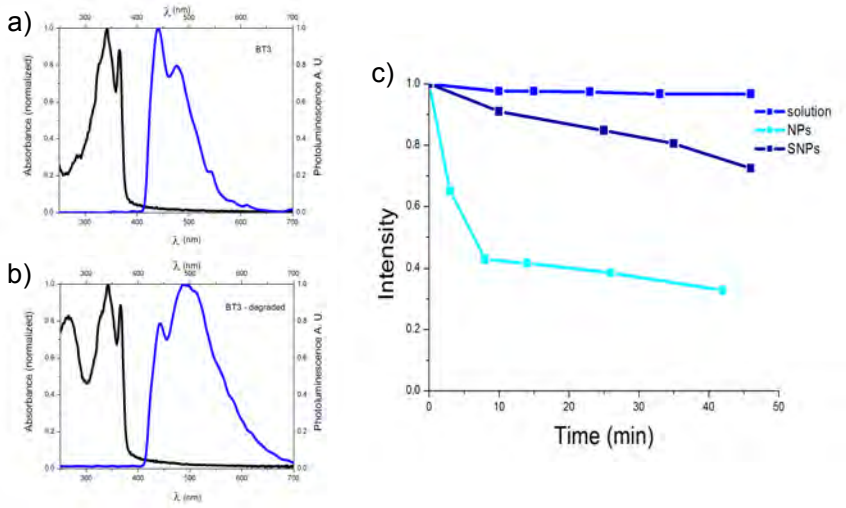

Figure B.2: BT3's degradation: absortion and photoluminiscence spectra of suspension at a) after preparing the suspension, b) one day after, approximately and c) comparation of degradation of BT3 in solution, NPs and SNPs.

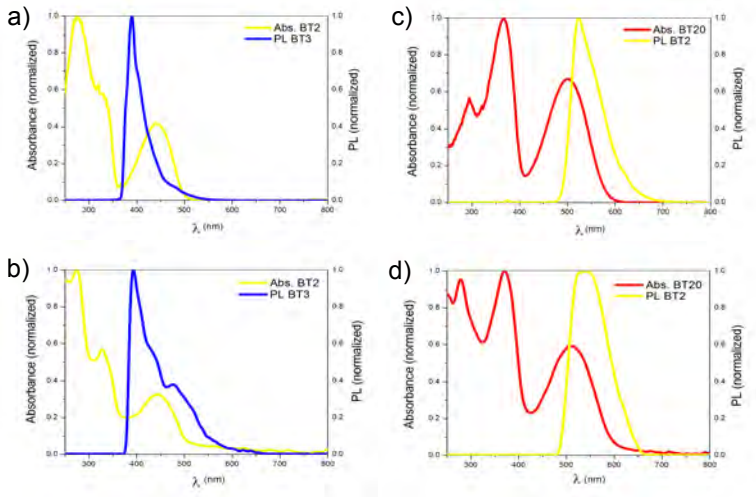

Figure B.3: The peak overlaps between PL and absorption spectra of RGBBTs emission materials; a) BT3→BT2 solution, b) BT3→BT2 NPs, c) BT2→BT20 solution, d) BT2→BT20 NPs.

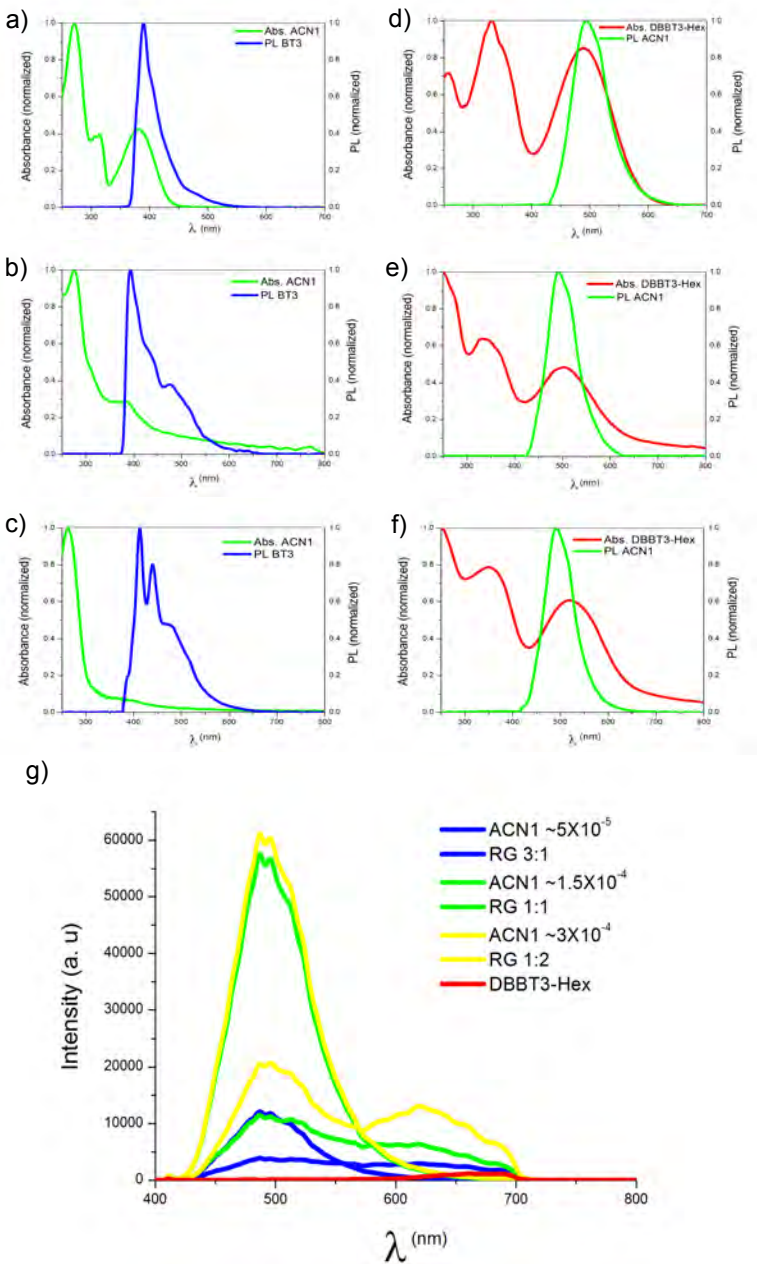

Figure B.4: The peak overlaps between PL and absorption spectra of RGB1 emission materials; a) BT3→ACN1 solution, b) BT3→ACN1 NPs, c) BT3→ACN1 SNPs, d) ACN1→DBBT3-Hex solution, e) ACN1→DBBT3-Hex NPs, f) ACN1→DBBT3-Hex SNPs and g) photoluminiscence spectra of ACN1, DBBT3-Hex and ACN1:DBBT3-Hex mixtures in suspension (NPs), changing the ACN1 concentration.

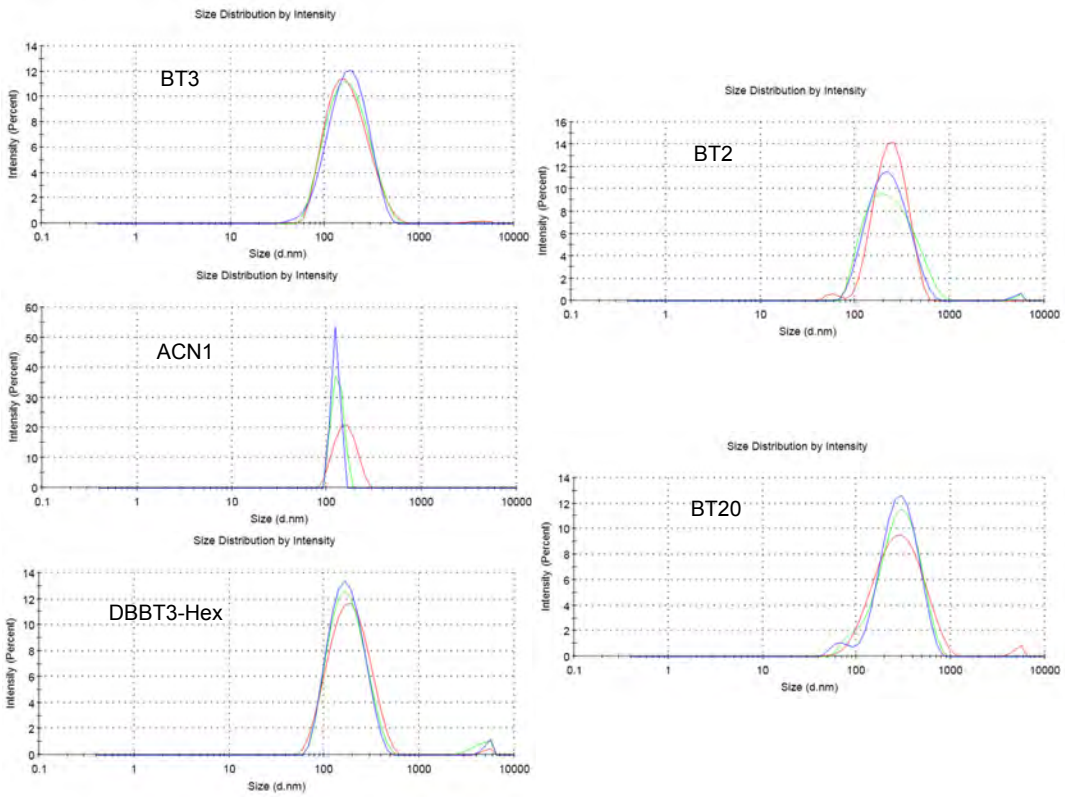

Figure B.5: Size distributions measured by DLS technique for the five molecules in suspension fabricated by reprecipitacion method.

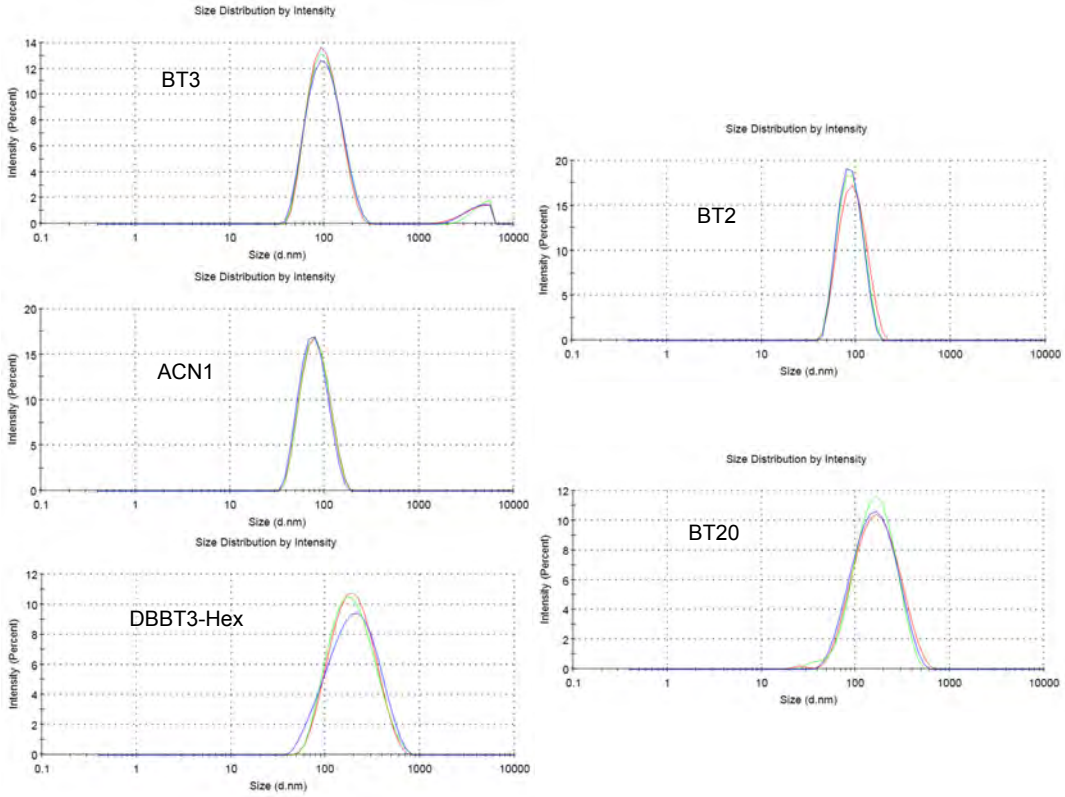

Figure B.6: Size distributions measured by DLS technique for the five molecules coated with silica fabricated by microemulsion method.

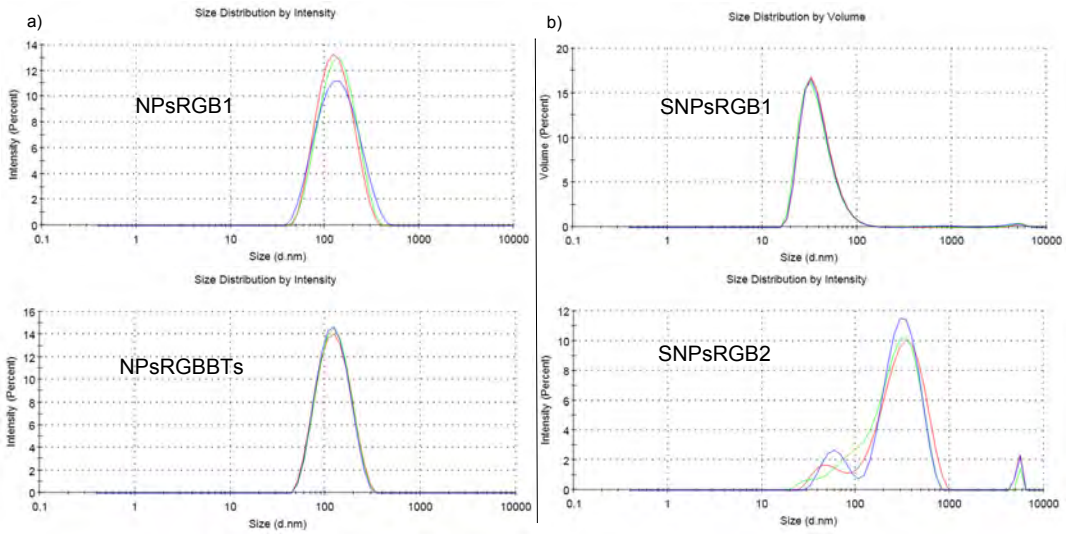

Figure B.7: Size distributions measured by DLS technique for a) DBBT3-Hex:ACN1:BT3 and BT20:BT2:BT3 mixtures by reprecipitacion method. b) DBBT3-Hex:ACN1:BT3 mixtures changing the ratio between them by microemulsion method.

Bibliography

[1] C. W. Tang and S. A. VanSlyke. Organic electroluminescent diodes. *Applied Physics Letters*, 51(12):913–915, 1987. doi: http://dx.doi.org/10.1063/1.98799. URL http://scitation.aip.org/content/aip/journal/apl/51/12/10.1063/1.98799.

[2] Adrien Kaeser and Albertus P. H. J. Schenning. Fluorescent nanoparticles based on self-assembled π-conjugated systems. *Advanced materials*, 22(28):2985–2997, 2010. doi: 10.1002/adma.201000427.

[3] Huibiao Liu, Jialiang Xu, Yongjun Li, and Yuliang Li. Aggregate nanostructures of organic molecular materials. *Accounts of chemical research*, 43(12):1496–1508, 2010.

[4] Otto S Wolfbeis. An overview of nanoparticles commonly used in fluorescent bioimaging. *Chemical Society Reviews*, 44(14):4743–4768, 2015. ISSN 0306-0012, 1460-4744. doi: 10.1039/C4CS00392F. URL http://xlink.rsc.org/?DOI=C4CS00392F.

[5] Ute Resch-Genger, Markus Grabolle, Sara Cavaliere-Jaricot, Roland Nitschke, and Thomas Nann. Quantum dots versus organic dyes as fluorescent labels. *Nature methods*, 5(9):763–775, 2008.

[6] Jin Zhang, Robert E Campbell, Alice Y Ting, and Roger Y Tsien. Creating new fluorescent probes for cell biology. *Nature Reviews Molecular Cell Biology*, 3(12):906–918, 2002.

[7] I. Hemmilä and V. Laitala. Progress in lanthanides as luminescent probes.

Journal of Fluorescence, 15(4):529–542, 2005. ISSN 1053-0509. doi: 10.1007/s10895-005-2826-6. URL http://dx.doi.org/10.1007/s10895-005-2826-6.

[8] Chun-Yi Sun, Xin-Long Wang, Xiao Zhang, Chao Qin, Peng Li, Zhong-Min Su, Dong-Xia Zhu, Guo-Gang Shan, Kui-Zhan Shao, Han Wu, et al. Efficient and tunable white-light emission of metal–organic frameworks by iridium-complex encapsulation. *Nature communications*, 4, 2013.

[9] Matthias IJ Stich, Lorenz H Fischer, and Otto S Wolfbeis. Multiple fluorescent chemical sensing and imaging. *Chemical Society Reviews*, 39(8):3102–3114, 2010.

[10] Xianfeng Zhou, Fengyu Su, Yanqing Tian, and Deirdre R Meldrum. Dually fluorescent core-shell microgels for ratiometric imaging in live antigen-presenting cells. *PloS one*, 9(2), 2014.

[11] Shang-Hsiu Hu and Xiaohu Gao. Nanocomposites with spatially separated functionalities for combined imaging and magnetolytic therapy. *Journal of the American Chemical Society*, 132(21):7234–7237, 2010. doi: 10.1021/ja102489q. URL http://dx.doi.org/10.1021/ja102489q. PMID: 20459132.

[12] Nathan C Shaner, Paul A Steinbach, and Roger Y Tsien. A guide to choosing fluorescent proteins. *Nature methods*, 2(12):905–909, 2005.

[13] Suzanne Fery-Forgues. Fluorescent organic nanocrystals and non-doped nanoparticles for biological applications. *Nanoscale*, 5(18):8428–8442, 2013.

[14] Yong Sheng Zhao, Hongbing Fu, Aidong Peng, Ying Ma, Debao Xiao, and Jiannian Yao. Low-dimensional nanomaterials based on small organic molecules: Preparation and optoelectronic properties. *Advanced Materials*, 20 (15):2859–2876, 2008. ISSN 1521-4095. doi: 10.1002/adma.200800604. URL http://dx.doi.org/10.1002/adma.200800604.

[15] Stephen R Forrest and Mark E Thompson. Introduction: organic electronics and optoelectronics. *Chemical Reviews*, 107(4):923–925, 2007.

[16] Partha Bairi, Bappaditya Roy, Priyadarshi Chakraborty, and Arun K Nandi. Co-assembled white-light-emitting hydrogel of melamine. *ACS applied materials & interfaces*, 5(12):5478–5485, 2013.

[17] Chakkooth Vijayakumar, Kazunori Sugiyasu, and Masayuki Takeuchi. Oligofluorene-based electrophoretic nanoparticles in aqueous medium as a donor scaffold for fluorescence resonance energy transfer and white-light emission. *Chemical Science*, 2(2):291–294, 2011.

[18] Junhong Zhou, Na Ai, Lei Wang, Hua Zheng, Chan Luo, Zhixiong Jiang, Shufu Yu, Yong Cao, and Jian Wang. Roughening the white OLED substrate's surface through sandblasting to improve the external quantum efficiency. *Organic Electronics*, 12(4):648–653, 2011.

[19] Leilei Tian Feng He Geng Chen b Fangzhong Shen Hong Xu Shumin Yang, Dan Lu and Yuguang Ma. Stable water-dispersed organic nanoparticles: preparation, optical properties, and cell imaging application. *Nanoscale*, 3(5):2261 – 2267, 2011. doi: 10.1039/c1nr10030k.

[20] Andrés Guerrero-Martínez, Jorge Pérez-Juste, and Luis M. Liz-Marzán. Recent progress on silica coating of nanoparticles and related nanomaterials. *Advanced Materials*, 22(11):1182–1195, 2010. ISSN 1521-4095. doi: 10.1002/adma.200901263. URL http://dx.doi.org/10.1002/adma.200901263.

[21] Ji Eon Kwon, Sanghyuk Park, and Soo Young Park. Realizing molecular pixel system for full-color fluorescence reproduction: RGB-emitting molecular mixture free from energy transfer crosstalk. *Journal of the American Chemical Society*, 135(30):11239–11246, 2013. doi: 10.1021/ja404256s. URL http://dx.doi.org/10.1021/ja404256s. PMID: 23876082.

[22] Lin Wang and Weihong Tan. Multicolor FRET silica nanoparticles by single wavelength excitation. *Nano letters*, 6(1):84–88, 2006.

[23] Hwan Myung Kim and Bong Rae Cho. Small-molecule two-photon probes for bioimaging applications. *Chemical Reviews*, 115(11):5014–5055, 2015. doi:

10.1021/cr5004425. URL http://dx.doi.org/10.1021/cr5004425. PMID: 25938620.

[24] Sehoon Kim, Tymish Y. Ohulchanskyy, Haridas E. Pudavar, Ravindra K. Pandey, and Paras N. Prasad. Organically modified silica nanoparticles co-encapsulating photosensitizing drug and aggregation-enhanced two-photon absorbing fluorescent dye aggregates for two-photon photodynamic therapy. *Journal of the American Chemical Society*, 129(9):2669–2675, 2007. doi: 10.1021/ja0680257. URL http://dx.doi.org/10.1021/ja0680257. PMID: 17288423.

[25] Malte C. Gather, Anne Köhnen, and Klaus Meerholz. White organic light-emitting diodes. *Advanced Materials*, 23(2):233–248, 2011. ISSN 1521-4095. doi: 10.1002/adma.201002636. URL http://dx.doi.org/10.1002/adma.201002636.

[26] Hak-Sung Jung, Young-Jae Kim, Shin-Woo Ha, and Jin-Kyu Lee. White light-emitting diodes using thermally and photochemically stable fluorescent silica nanoparticles as color-converters. *Journal of Materials Chemistry C*, 1(37): 5879–5884, 2013.

[27] Carlo Giansante, Christian Schäfer, Guillaume Raffy, and André Del Guerzo. Exploiting direct and cascade energy transfer for color-tunable and white-light emission in three-component self-assembled nanofibers. *The Journal of Physical Chemistry C*, 116(41):21706–21716, 2012. doi: 10.1021/jp3073188. URL http://dx.doi.org/10.1021/jp3073188.

[28] Yilong Lei, Qing Liao, Hongbing Fu, and Jiannian Yao. Orange−blue−orange triblock one-dimensional heterostructures of organic microrods for white-light emission. *Journal of the American Chemical Society*, 132(6):1742–1743, 2010. doi: 10.1021/ja9084435. URL http://dx.doi.org/10.1021/ja9084435. PMID: 20102187.

[29] Jeremy Malinge, Clémence Allain, Arnaud Brosseau, and Pierre Audebert. White fluorescence from core–shell silica nanoparticles. *Angewandte Chemie International Edition*, 51(34):8534–8537, 2012. ISSN 1521-3773. doi: 10.1002/anie.201203374. URL http://dx.doi.org/10.1002/anie.201203374.

[30] Youjun Yang, * Mark Lowry, Corin M. Schowalter, Sayo O. Fakayode, Jorge O. Escobedo, Xiangyang Xu, Huating Zhang, Timothy J. Jensen, Frank R. Fronczek, * Isiah M. Warner, , and Robert M. Strongin*. An organic white light-emitting fluorophore. *Journal of the American Chemical Society*, 128(43): 14081–14092, 2006. doi: 10.1021/ja0632207. URL http://dx.doi.org/10.1021/ja0632207. PMID: 17061891.

[31] Mijanur Rahaman Molla, Dominik Gehrig, Lisa Roy, Valentin Kamm, Ankan Paul, Frédéric Laquai, and Suhrit Ghosh. Self-assembly of carboxylic acid appended naphthalene diimide derivatives with tunable luminescent color and electrical conductivity. *Chemistry – A European Journal*, 20(3):760–771, 2014. ISSN 1521-3765. doi: 10.1002/chem.201303379. URL http://dx.doi.org/10.1002/chem.201303379.

[32] Sanjoy Mukherjee and Pakkirisamy Thilagar. Organic white-light emitting materials. *Dyes and Pigments*, 110(0):2 – 27, 2014. doi: http://dx.doi.org/10.1016/j.dyepig.2014.05.031. URL http://www.sciencedirect.com/science/article/pii/S0143720814002198.

[33] Diecenia Peralta-Domínguez, Mario Rodríguez, Gabriel Ramos-Ortíz, José Luis Maldonado, Marco A. Meneses-Nava, Oracio Barbosa-García, Rosa Santillan, and Norberto Farfán. A schiff base derivative from cinnamaldehyde for colorimetric detection of ni2+ in water. *Sensors and Actuators B: Chemical*, 207, Part A(0):511 – 517, 2015. ISSN 0925-4005. doi: http://dx.doi.org/10.1016/j.snb.2014.09.100. URL http://www.sciencedirect.com/science/article/pii/S0925400514011903.

[34] Daniel Romero-Borja, José-Luis Maldonado, Oracio Barbosa-García, Mario Rodríguez, Enrique Pérez-Gutiérrez, Rosalba Fuentes-Ramírez, and Guadalupe de la Rosa. Polymer solar cells based on P3HT:PC71BM doped at different concentrations of isocyanate-treated graphene. *Synthetic Metals*, 200(0): 91 – 98, 2015. ISSN 0379-6779. doi: http://dx.doi.org/10.1016/j.synthmet.2014.12.029. URL http://www.sciencedirect.com/science/article/pii/S0379677914004639.

[35] Dan Chi, Shengchun Qu, Zhanguo Wang, and Jizheng Wang. High efficiency P3HT:PCBM solar cells with an inserted pcbm layer. *J. Mater. Chem. C*, 2: 4383–4387, 2014. doi: 10.1039/C4TC00003J. URL http://dx.doi.org/10.1039/C4TC00003J.

[36] Jeremy J. Intemann, Kai Yao, Hin-Lap Yip, Yun-Xiang Xu, Yong-Xi Li, Po-Wei Liang, Fei-Zhi Ding, Xiaosong Li, and Alex K.-Y. Jen. Molecular weight effect on the absorption, charge carrier mobility, and photovoltaic performance of an indacenodiselenophene-based ladder-type polymer. *Chemistry of Materials*, 25 (15):3188–3195, 2013. doi: 10.1021/cm401586t. URL http://dx.doi.org/10.1021/cm401586t.

[37] Sybille Allard, Michael Forster, Benjamin Souharce, Heiko Thiem, and Ullrich Scherf. Organic semiconductors for solution-processable field-effect transistors (OFETs). *Angewandte Chemie International Edition*, 47(22):4070–4098, 2008. ISSN 1521-3773. doi: 10.1002/anie.200701920. URL http://dx.doi.org/10.1002/anie.200701920.

[38] Shumin Yang, Dan Lu, Leilei Tian, Feng He, Geng Chen, Fangzhong Shen, Hong Xu, and Yuguang Ma. Stable water-dispersed organic nanoparticles: preparation, optical properties, and cell imaging application. *Nanoscale*, 3(5): 2261–2267, 2011.

[39] Xiaoyu Zhang, Yu Zhang, Yu Wang, Sergii Kalytchuk, Stephen V. Kershaw, Yinghui Wang, Peng Wang, Tieqiang Zhang, Yi Zhao, Hanzhuang Zhang, Tian Cui, Yiding Wang, Jun Zhao, William W. Yu, and Andrey L. Rogach. Color-switchable electroluminescence of carbon dot light-emitting diodes. *ACS NANO*, 7(12):11234–11241, 2013.

[40] Bingxin Liu, Xiaodan Lü, Chunyu Wang, Cuiyan Tong, Yao He, and Changli Lü. White light emission transparent polymer nanocomposites with novel poly(p-phenylene vinylene) derivatives and surface functionalized cdse/zns NCs. *Dyes and Pigments*, 99(1):192 – 200, 2013. ISSN 0143-7208. doi: http://dx.doi.org/10.1016/j.dyepig.2013.04.038. URL http://www.sciencedirect.com/science/article/pii/S0143720813001678.

[41] Zhenzhen Xu, Qing Liao, Xingrui Shi, Hui Li, Haoli Zhang, and Hongbing Fu. Full-color tunable organic nanoparticles with FRET-assisted enhanced two-photon excited fluorescence for bio-imaging. *J. Mater. Chem. B*, 1: 6035–6041, 2013. doi: 10.1039/C3TB20841A. URL http://dx.doi.org/10.1039/C3TB20841A.

[42] Yi Han, Hong-Tao Cao, Hai-Zhu Sun, Yong Wu, Guo-Gang Shan, Zhong-Min Su, Xue-Gang Hou, and Yi Liao. Effect of alkyl chain length on piezochromic luminescence of iridium(iii)-based phosphors adopting 2-phenyl-1h-benzoimidazole type ligands. *J. Mater. Chem. C*, 2:7648–7655, 2014. doi: 10.1039/C4TC00993B. URL http://dx.doi.org/10.1039/C4TC00993B.

[43] Hong-Zhi Tang, Michiya Fujiki, and Masao Motonaga. Alkyl side chain effects of optically active polyfluorenes on their chiroptical absorption and emission properties. *Polymer*, 43(23):6213 – 6220, 2002. ISSN 0032-3861. doi: http://dx.doi.org/10.1016/S0032-3861(02)00581-5. URL http://www.sciencedirect.com/science/article/pii/S0032386102005815.

[44] Veronika Hrobáriková, Peter Hrobárik, Peter Gajdoš, Ioannis Fitilis, Mihalis Fakis, Peter Persephonis, and Pavol Zahradnîk. Benzothiazole-based fluorophores of donor-π-acceptor-π-donor type displaying high two-photon absorption. *The Journal of organic chemistry*, 75(9):3053–3068, 2010.

[45] Stephanie JK Pond, Mariacristina Rumi, Michael D Levin, Timothy C Parker, David Beljonne, Michael W Day, Jean-Luc Brédas, Seth R Marder, and Joseph W Perry. One-and two-photon spectroscopy of donor-acceptor-donor distyrylbenzene derivatives: effect of cyano substitution and distortion from planarity. *The Journal of Physical Chemistry A*, 106(47):11470–11480, 2002.

[46] Mariacristina Rumi, Jeffrey E. Ehrlich, Ahmed A. Heikal, Joseph W. Perry, Stephen Barlow, Zhongying Hu, Dianne McCord-Maughon, Timothy C. Parker, Harald Röckel, Sankaran Thayumanavan, Seth R. Marder, David Beljonne, and Jean-Luc Brédas. Structure−property relationships for two-photon absorbing chromophores: bis-donor diphenylpolyene and bis(styryl)benzene derivatives.

Journal of the American Chemical Society, 122(39):9500–9510, 2000. doi: 10.1021/ja994497s. URL http://dx.doi.org/10.1021/ja994497s.

[47] Chetan Bhongale and Chain-Shu Hsu. *Organic Nanoparticles and Organic-Inorganic Hybrid Nanocomposites*. WILEY-VCH Verlag GmbH & Co. KGaA, 2011.

[48] G.G. Guilbault. *Practical Fluorescence, Second Edition*. Modern Monographs in Analytical Chemistry. Taylor & Francis, 1990. ISBN 9780824783501. URL https://books.google.com.mx/books?id=7eI3AVl4dDsC.

[49] Joseph R. Lakowicz, editor. *Principles of fluorescence spectroscopy*. second edition.

[50] Bo Li, Tomonori Kawakami, and Mitsuo Hiramatsu. Enhancement of organic nanoparticle preparation by laser ablation in aqueous solution using surfactants. *Applied Surface Science*, 210(3–4):171 – 176, 2003. ISSN 0169-4332. doi: http://dx.doi.org/10.1016/S0169-4332(03)00009-6. URL http://www.sciencedirect.com/science/article/pii/S0169433203000096.

[51] Yoshiaki Tamaki, Tsuyoshi Asahi, and Hiroshi Masuhara. Nanoparticle formation of vanadyl phthalocyanine by laser ablation of its crystalline powder in a poor solvent†. *The Journal of Physical Chemistry A*, 106(10):2135–2139, 2002. doi: 10.1021/jp012518a. URL http://dx.doi.org/10.1021/jp012518a.

[52] Vincenzo Amendola and Moreno Meneghetti. Laser ablation synthesis in solution and size manipulation of noble metal nanoparticles. *Physical chemistry chemical physics*, 11(20):3805–3821, 2009.

[53] T. Asahi, T. Sugiyama, and H. Masuhara. Laser fabrication and spectroscopy of organic nanoparticles. *Accounts of Chemical Research*, 41(12):1790–1798, 2008. doi: 10.1021/ar800125s. URL http://dx.doi.org/10.1021/ar800125s. PMID: 18937507.

[54] Chih-Chia Huang, Chen-Sheng Yeh, and Ching-Jeng Ho. Laser ablation synthesis of spindle-like gallium oxide hydroxide nanoparticles with the pres-

ence of cationic cetyltrimethylammonium bromide. *The Journal of Physical Chemistry B*, 108(16):4940–4945, 2004. doi: 10.1021/jp037427n. URL http://dx.doi.org/10.1021/jp037427n.

[55] M. Lal, L. Levy, K. S. Kim, G. S. He, X. Wang, Y. H. Min, S. Pakatchi, and P. N. Prasad. Silica nanobubbles containing an organic dye in a multilayered organic/inorganic heterostructure with enhanced luminescence. *Chemistry of Materials*, 12(9):2632–2639, 2000. doi: 10.1021/cm000178k. URL http://dx.doi.org/10.1021/cm000178k.

[56] Yijun Yu, Bo Che, Zhihua Si, Liang Li, Wei Chen, and Gi Xue. Carbon nanotube/polyaniline core-shell nanowires prepared by in situ inverse microemulsion. *Synthetic Metals*, 150(3):271 – 277, 2005. ISSN 0379-6779. doi: http://dx.doi.org/10.1016/j.synthmet.2005.02.011. URL http://www.sciencedirect.com/science/article/pii/S0379677905000949.

[57] Maqsood Ahmad Malik, Mohammad Younus Wani, and Mohd Ali Hashim. Microemulsion method: A novel route to synthesize organic and inorganic nanomaterials: 1st nano update. *Arabian Journal of Chemistry*, 5(4):397 – 417, 2012. ISSN 1878-5352. doi: http://dx.doi.org/10.1016/j.arabjc.2010.09.027. URL http://www.sciencedirect.com/science/article/pii/S1878535210002005.

[58] M.Arturo López-Quintela. Synthesis of nanomaterials in microemulsions: formation mechanisms and growth control. *Current Opinion in Colloid & Interface Science*, 8(2):137 – 144, 2003. ISSN 1359-0294. doi: http://dx.doi.org/10.1016/S1359-0294(03)00019-0. URL http://www.sciencedirect.com/science/article/pii/S1359029403000190.

[59] F. Debuigne, L. Jeunieau, M. Wiame, and J. B.Nagy. Synthesis of organic nanoparticles in different w/o microemulsions. *Langmuir*, 16(20):7605–7611, 2000. doi: 10.1021/la991638v. URL http://dx.doi.org/10.1021/la991638v.

[60] Su-Hua Yang, Po-Jen Shih, Wen-Jie Wu, and Yi-Hua Huang. Color-tunable and stable-efficiency white organic light-emitting diode fabricated with

fluorescent-phosphorescent emission layers. *Journal of Luminescence*, 142(0): 86 – 91, 2013. ISSN 0022-2313. doi: http://dx.doi.org/10.1016/j.jlumin.2013.03.060. URL http://www.sciencedirect.com/science/article/pii/S0022231313002007.

[61] R.S. Berns, F.W. Billmeyer, and M. Saltzman. *Billmeyer and Saltzman's principles of color technology*. Wiley-Interscience publication. Wiley, 2000. ISBN 9780471194590. URL https://books.google.com.mx/books?id=Ss_vAAAAMAAJ.

[62] N. Ohta and A. Robertson. *Colorimetry: Fundamentals and Applications*. The Wiley-IS&T Series in Imaging Science and Technology. Wiley, 2006. ISBN 9780470094730. URL https://books.google.com.mx/books?id=U8jeh1uhSHgC.

[63] Kiran T. Kamtekar, Andrew P. Monkman, and Martin R. Bryce. Recent advances in white organic light-emitting materials and devices (WOLEDs). *Advanced Materials*, 22(5):572–582, 2010. ISSN 1521-4095. doi: 10.1002/adma.200902148. URL http://dx.doi.org/10.1002/adma.200902148.

[64] Kai Li and Bin Liu. Polymer-encapsulated organic nanoparticles for fluorescence and photoacoustic imaging. *Chemical Society Reviews*, 43(18):6570–6597, 2014.

[65] Tsutomu Ishi-i, Kei Ikeda, Yuki Kichise, and Michiaki Ogawa. Red-light-emitting system based on aggregation of donor–acceptor derivatives in polar aqueous media. *Chemistry – An Asian Journal*, 7(7):1553–1557, 2012. ISSN 1861-471X. doi: 10.1002/asia.201200136. URL http://dx.doi.org/10.1002/asia.201200136.

[66] Jesús Rodríguez-Romero, Laura Aparicio-Ixta, Mario Rodríguez, Gabriel Ramos-Ortíz, José Luis Maldonado, Arturo Jiménez-Sánchez, Norberto Farfán, and Rosa Santillan. Synthesis, chemical–optical characterization and solvent interaction effect of novel fluorene-chromophores with d-a-d structure. *Dyes and Pigments*, 98(1):31–41, 2013.

[67] Axel D. Becke. Density-functional thermochemistry. iii. the role of exact exchange. *The Journal of Chemical Physics*, 98(7):5648–5652, 1993. doi: http://dx.doi.org/10.1063/1.464913. URL http://scitation.aip.org/content/aip/journal/jcp/98/7/10.1063/1.464913.

[68] Michelle M Francl, William J Pietro, Warren J Hehre, J Stephen Binkley, Mark S Gordon, Douglas J DeFrees, and John A Pople. Self-consistent molecular orbital methods. xxiii. a polarization-type basis set for second-row elements. *The Journal of Chemical Physics*, 77(7):3654–3665, 1982.

[69] M. J. Frisch, G. W. Trucks, H. B. Schlegel, G. E. Scuseria, M. A. Robb, J. R. Cheeseman, G. Scalmani, V. Barone, B. Mennucci, G. A. Petersson, H. Nakatsuji, M. Caricato, X. Li, H. P. Hratchian, A. F. Izmaylov, J. Bloino, G. Zheng, J. L. Sonnenberg, M. Hada, M. Ehara, K. Toyota, R. Fukuda, J. Hasegawa, M. Ishida, T. Nakajima, Y. Honda, O. Kitao, H. Nakai, T. Vreven, J. A. Montgomery, J. E. Peralta, F. Ogliaro, M. Bearpark, J. J. Heyd, E. Brothers, K. N. Kudin, V. N. Staroverov, R. Kobayashi, J. Normand, K. Raghavachari, A. Rendell, J. C. Burant, S. S. Iyengar, J. Tomasi, M. Cossi, N. Rega, J. M. Millam, M. Klene, J. E. Knox, J. B. Cross, V. Bakken, C. Adamo, J. Jaramillo, R. Gomperts, R. E. Stratmann, O. Yazyev, A. J. Austin, R. Cammi, C. Pomelli, J. W. Ochterski, R. L. Martin, K. Morokuma, V. G. Zakrzewski, G. A. Voth, P. Salvador, J. J. Dannenberg, S. Dapprich, A. D. Daniels, Farkas, J. B. Foresman, J. V. Ortiz, J. Cioslowski, and D. J. Fox. Gaussian 09, Revision B.01, 2009.

[70] P.C. Hariharan and J.A. Pople. The influence of polarization functions on molecular orbital hydrogenation energies. *Theoretica chimica acta*, 28(3): 213–222, 1973. ISSN 0040-5744. doi: 10.1007/BF00533485. URL http://dx.doi.org/10.1007/BF00533485.

[71] W. J. Hehre, R. Ditchfield, and J. A. Pople. Self—consistent molecular orbital methods. xii. further extensions of gaussian—type basis sets for use in molecular orbital studies of organic molecules. *The Journal of Chemical Physics*, 56(5), 1972.

[72] Chengteh Lee, Weitao Yang, and Robert G. Parr. Development of the colle-

salvetti correlation-energy formula into a functional of the electron density. *Phys. Rev. B*, 37:785–789, Jan 1988. doi: 10.1103/PhysRevB.37.785. URL http://link.aps.org/doi/10.1103/PhysRevB.37.785.

[73] C Estupiñán-López, C Tolentino Dominguez, and RE de Araujo. Eclipsing thermal lens spectroscopy for fluorescence quantum yield measurement. *Optics express*, 21(15):18592–18601, 2013.

[74] Albert M Brouwer. Standards for photoluminescence quantum yield measurements in solution (iupac technical report). *Pure and Applied Chemistry*, 83(12): 2213–2228, 2011.

[75] Longtian Kang, Yu Chen, Debao Xiao, Aidong Peng, Fugang Shen, Xun Kuang, Hongbing Fu, and Jiannian Yao. Organic core/diffuse-shell nanorods: fabrication, characterization and energy transfer. *Chemical Communications*, (26): 2695–2697, 2007.

[76] A.-D. Peng, D.-B. Xiao, Y. Ma, W.-S. Yang, and J.-N. Yao. Tunable emission from doped 1,3,5-triphenyl-2-pyrazoline organic nanoparticles. *Advanced Materials*, 17(17):2070–2073, 2005. ISSN 1521-4095. doi: 10.1002/adma.200401989. URL http://dx.doi.org/10.1002/adma.200401989.

[77] Fu Tang, Chun Wang, Jinshan Wang, Xiaoyu Wang, and Lidong Li. Fluorescent organic nanoparticles with enhanced fluorescence by self-aggregation and their application to cellular imaging. *ACS Applied Materials & Interfaces*, 6(20): 18337–18343, 2014. doi: 10.1021/am505776a. URL http://dx.doi.org/10.1021/am505776a. PMID: 25275214.

[78] Aparicio-Ixta G. Ramos-Ortiz J. L. Pichardo-Molina J. L. Maldonado M. Rodríguez V. M. Tellez-Lopez D. Martinez-Fong M. G. Zolotukhin S. Fomine M. A. Meneses-Nava O. Barbosa-García L. Two-photon excited fluorescence of silica nanoparticles loaded with a fluorene-based monomer and its crossconjugated polymer: their application to cell imaging. *Nanoscale*, 4:7751 – 7759, 2012.

[79] Chao Tang, Xu-Dong Liu, Feng Liu, Xu-Liang Wang, Hui Xu, and Wei Huang. Recent progress in polymer white light-emitting materials and de-

vices. *Macromolecular Chemistry and Physics*, 214(3):314–342, 2013. ISSN 1521-3935. doi: 10.1002/macp.201200305. URL http://dx.doi.org/10.1002/macp.201200305.

[80] Miłosz Pawlicki, Hazel A. Collins, Robert G. Denning, and Harry L. Anderson. Two-photon absorption and the design of two-photon dyes. *Angewandte Chemie International Edition*, 48(18):3244–3266, 2009. ISSN 1521-3773. doi: 10.1002/anie.200805257. URL http://dx.doi.org/10.1002/anie.200805257.

[81] Sébastien Thiery, Eline Declairieux, Denis Tondelier, Gijun Seo, Bernard Geffroy, Olivier Jeannin, Rémi Métivier, Cyril Poriel, and J Rault-Berthelot. 2-substituted vs 4-substituted-9,9'-spirobifluorene host materials for green and blue phosphorescent oleds: a structureeproperty relationship study. *Elsevier*, 70:6337–6351, 2014.

[82] Yalong Wang, Tongliang Liu, Lingyu Bu, Jinfeng Li, Chao Yang, Xiaojing Li, Yong Tao, and Wenjun Yang. Aqueous nanoaggregation-enhanced one- and two-photon fluorescence, crystalline j-aggregation-induced red shift, and amplified spontaneous emission of 9,10-bis(p-dimethylaminostyryl)anthracene. *The Journal of Physical Chemistry C*, 116(29):15576–15583, 2012. doi: 10.1021/jp3031094. URL http://dx.doi.org/10.1021/jp3031094.

[83] Linlin Liu, Shi Tang, Meirong Liu, Zengqi Xie, Wu Zhang, Ping Lu, Muddasir Hanif, and Yuguang Ma. Photodegradation of polyfluorene and fluorene oligomers with alkyl and aromatic disubstitutions. *The Journal of Physical Chemistry B*, 110(28):13734–13740, 2006. doi: 10.1021/jp062612x. URL http://dx.doi.org/10.1021/jp062612x. PMID: 16836318.

[84] Marian Asantewah Nkansah. Preliminary photochemical studies of fluorene in various aqueous media. 5(3):97–103, 2014.

[85] Nam Ho Kim, You-Hyun Kim, Ju-An Yoon, Sang Youn Lee, Dae Hyun Ryu, Richard Wood, C.-B. Moon, and Woo Young Kim. Color optimization of single emissive white OLEDs via energy transfer between RGB fluorescent dopants. *Journal of Luminescence*, 143(0):723 – 728, 2013. ISSN 0022-2313. doi: http:

//dx.doi.org/10.1016/j.jlumin.2013.05.048. URL http://www.sciencedirect.com/science/article/pii/S0022231313003293.

[86] X. Zhu, D.-H. Lee, H. Chae, and S.M. Cho. Abrupt change of luminescence spectrum in single-layer phosphorescent polymer light emitting diode. *Journal of Luminescence*, 132(1):12 – 15, 2012. ISSN 0022-2313. doi: http://dx.doi.org/10.1016/j.jlumin.2011.07.019. URL http://www.sciencedirect.com/science/article/pii/S0022231311004340.

[87] J. Schanda. *Colorimetry: Understanding the CIE System*. Wiley, 2007. ISBN 9780470175620.

[88] K. Nassau. *The physics and chemistry of color: the fifteen causes of color*. Wiley series in pure and applied optics. Wiley, 2001. ISBN 9780471391067. URL https://books.google.com.mx/books?id=oasPAQAAMAAJ.

[89] Hongzhen Lin and Fenglian Bai. Electronic process in organic solids, 2013.

[90] Frédéric Laquai, Young-Seo Park, Jang-Joo Kim, and Thomas Basché. Excitation energy transfer in organic materials: From fundamentals to optoelectronic devices. *Macromolecular rapid communications*, 30(14):1203–1231, 2009.

[91] Gregory D. Scholes. Long-range resonance energy transfer in molecular systems. *Annual review of physical chemistry*, 54(1):57–87, 2003.

[92] Bernard Valeur and Mário Nuno Berberan-Santos. *Excitation Energy Transfer*, pages 213–261. Wiley-VCH Verlag GmbH & Co. KGaA, 2012. ISBN 9783527650002. doi: 10.1002/9783527650002.ch8. URL http://dx.doi.org/10.1002/9783527650002.ch8.